

# **CO<sub>2</sub> multicyclic capture of pretreated/doped CaO in the Ca-looping process. Theory and experiments**

Jose M. Valverde<sup>a</sup>, Pedro E. Sanchez-Jimenez<sup>b</sup>, Antonio Perejon<sup>b</sup>, Luis A. Perez-Maqueda<sup>b</sup>

<sup>a</sup> Faculty of Physics. University of Seville. Avenida Reina Mercedes s/n, 41012 Sevilla, Spain

<sup>b</sup> Institute of Materials Science (CSIC-University of  
Seville) Americo Vespucio 49, 41092 Sevilla, Spain.

## Abstract

We study in this paper the conversion of CaO-based CO<sub>2</sub> sorbents when subjected to repeated carbonation/calcination cycles with a focus on thermally pretreated/doped sorbents. Analytical equations are derived to describe the evolution of conversion with the cycle number from a unifying model based on the balance between surface area loss due to sintering in the looping-calcination stage and surface area regeneration as a consequence of solid-state diffusion during the looping-carbonation stage. Multicyclic CaO conversion is governed by the evolution of surface area loss/regeneration that strongly depends on the initial state of the pore skeleton. In the case of thermally pretreated sorbents, the initial pore skeleton is highly sintered and regeneration is relevant whereas, for nonpretreated sorbents, the initial pore skeleton is soft and regeneration is negligible. Experimental results are obtained for sorbents subjected to a preheating controlled rate thermal analysis (CRTA) program. By applying this preheating program in a CO<sub>2</sub> enriched atmosphere, CaO can be subjected to a rapid carbonation followed by a slow rate controlled decarbonation, which yields a highly sintered skeleton displaying a small conversion in the first cycle and self-reactivation in the next ones. Conversely, carbonation of the sorbent at a slow controlled rate enhances CO<sub>2</sub> solid-state diffusion, which gives rise, after a quick decarbonation, to a highly porous skeleton. In this case, CaO conversion in the first cycle is very large but it decays abruptly in subsequent cycles. Data on CaO conversion retrieved from the literature and from further experimental measurements performed in our work are analyzed as influenced by a variety of experimental variables such as preheating temperature program, preheating exposition time, atmosphere composition, presence of additives, and carbonation/calcination conditions. Conversion data are well fitted by the proposed model equations, which are of help for a quantitative interpretation on the effect of experimental conditions on the multicyclic sorbent performance as a function of sintering/regeneration parameters inferred from the fittings and allow foreseeing the critical conditions to promote reactivation. The peculiar behavior of some pretreated sorbents, showing a maximum of conversion at a small number of cycles, is explained in the light of the model.

## I. INTRODUCTION

The Ca-looping (CaL) technology to capture  $\text{CO}_2$  is based on the carbonation of  $\text{CaO}$  and the subsequent decomposition of  $\text{CaCO}_3$  by calcination to regenerate the sorbent in order to be reused in a long-series cyclic process [1, 2]. As it has been demonstrated from the proved efficiency of large pilot-scale plants, with sustained  $\text{CO}_2$  capture efficiencies over 90% [3], the CaL technology has a considerable potential for reducing postcombustion  $\text{CO}_2$  emissions from industrial-scale power plants in the short-term. In practice, carbonation/calcination cycles are realized by means of two interconnected fluidized beds. The  $\text{CaO}$  particles react in a fluidized bed reactor (carbonator) with the  $\text{CO}_2$  in the fluidizing postcombustion. Carbonated particles are then circulated into a second fluidized bed reactor (calciner). In the calciner,  $\text{CaCO}_3$  decomposes to yield  $\text{CaO}$  and a pure dry stream of  $\text{CO}_2$ , which is suitable to be compressed and transported for sequestration. By taking into account the tradeoff between the reaction equilibrium driving force and the reaction kinetics, carbonation is carried out at optimal temperatures around  $650^\circ\text{C}$ . On the other hand, oxyfired combustion is carried out in the calciner by burning coal with a stream of pure  $\text{O}_2$  in order to supply the necessary heat for decarbonation and to produce a sufficiently high concentrated stream of  $\text{CO}_2$  for purification and compression. High concentrations of  $\text{CO}_2$  in the calciner requires temperatures above  $900^\circ\text{C}$  for decarbonation to occur at practical rates [4].

Lu et al. [5] have analyzed the  $\text{CO}_2$  capture performance of  $\text{CaO}$  sorbents obtained from different precursors such as calcium nitrate, calcium hydroxide, limestone, and calcium acetate monohydrate. Even though  $\text{CaO}$  prepared from calcium acetate monohydrate has been identified as the best performing sorbent, natural limestones are considered as the most suitable candidates to be employed in industrial applications due to their low price, wide availability, easy handling, and recyclability in the cement industry [6–9]. Thermogravimetric analysis (TGA) studies have shown that carbonation of  $\text{CaO}$  particles takes place in two well differentiated phases [10, 11]. Firstly,  $\text{CO}_2$  is quickly chemisorbed on the free surface of  $\text{CaO}$  until a thin layer of  $\text{CaCO}_3$  (between 30 and 50 nm thick [11]) covers it. Then, carbonation turns to be controlled by solid-state diffusion of  $\text{CO}_2$  through this layer, which is a slow process. In an ideal scenario, nascent  $\text{CaO}$  from limestone should react mostly in the fast carbonation phase to achieve a maximum  $\text{CaO}$  conversion that should be kept as high as possible in subsequent cycles. However, natural limestones suffer a marked loss of  $\text{CaO}$

conversion as they are subjected to repeated carbonation/calcination cycles [10] converging to a residual value below 0.1 (ratio of converted CaO mass to initial CaO mass) [12]. High solids circulation rates in pilot scale plants may compensate for this low residual conversion while still allowing the technology to be economically feasible [6, 13]. Nonetheless, the enhancement of sorbent regenerability would suppose an additional benefit to improve the competitiveness of the CaL technology [8, 13].

may compensate for this low residual conversion while still allowing the technology to be economically feasible.

The decay of CaO conversion with the number of carbonation/calcination cycles is essentially due to the progressive sintering suffered during the looping calcination stage by the initial soft skeleton [10]. CaO sintering causes a decrease of the available surface area for fast carbonation, which leads to a decrease of short-timed conversion in the successive carbonation. The addition of dopants, with higher thermal stability, is a direction of research to improve the regenerability of limestones (see [14, 15] for recent reviews). CaO synthetic sorbents have been also formulated by using dopants that increase the affinity towards CO<sub>2</sub> such as alkali metals [16]. Other widely investigated strategies to enhance the regenerability of natural limestones are hydration and thermal pretreatment [1]. The latter will be a subject of interest in the present manuscript.

Usually, multicyclic CaO conversion is assessed in TGA experiments, where CaO is derived by calcining its precursor. Calcination temperature and duration must be large enough to ensure that decarbonation is complete but, in order to ensure maximum sorption efficiency, not excessively high to avoid that the CaO grains sinter after formation. A radically different approach is pursued by the thermal pretreatment technique. Thermal pretreatment of natural limestones was first examined by Manovic and Anthony [17], who observed a beneficial effect of prolonged exposure of the sorbent to isothermal calcination at high temperature on the subsequent evolution of the multicyclic CaO conversion. In the case of limestones severely sintered by very long preheating periods and/or very high temperatures, CaO conversion actually increased in the first cycles, which was referred to as self-reactivation [17]. Self-reactivation exhibited by thermally pretreated limestones has been reported in many works in the last years [17–23]. Even though recent advances [8, 24] have been made to model self-reactivation, some characteristic features of this type of behavior remain still to be explained such as the existence of a maximum of conversion at a certain number of

cycles. In the present manuscript a quantitative analysis of self-activation will be carried out to help rationalize this peculiar type of behavior. Experimental results on CaO multicyclic conversion reported in the literature as affected by a diversity of conditions, as well as experimental data obtained in our work, will be analyzed in the light of a proposed model.

## II. MODELS ON MULTICYCLIC CAO CONVERSION

Deactivation of CaO during multiple carbonation/calcination cycles is reminiscent of the sintering induced loss of surface area observed for supported metal catalysts. According to extensive BET surface area measurements reported in the literature reviewed by Bartholomew [25], the decrease of the catalyst surface area  $S$  conforms generally to the empirical rate equation

$$-\frac{d}{dt} \left( \frac{S}{S_0} \right) = \kappa \left( \frac{S}{S_0} \right)^n \quad (1)$$

where  $S_0$  is the initial surface area,  $\kappa$  is the sintering rate constant, and  $n$  is the so-called sintering order. Equation 1, which is known as the simple power law expression (SPLE), was justified from the assumption that surface energy provides the driving force for sintering [26]. However, the sintering order is found to vary in a wide range between 3 and 15 [27] being usually a function of time, temperature and atmosphere, which rests confidence to its use [25].

In order to employ Eq. 1 to describe multicyclic CaO conversion, it is assumed that, in the CaL process, conversion at the  $i$ th carbonation  $X_i$  is proportional to the available surface area for reacting with  $\text{CO}_2$  ( $X_i/X_0 \propto S_i/S_0$ , where  $X_0$  is the CaO conversion in the first carbonation  $i = 0$ ). Using a differential approach it is

$$-\int_{X_0}^{X_N} \frac{dX}{X^n} = \int_0^N \kappa di \quad (2)$$

which leads to

$$X_N = \left[ \frac{1}{\kappa N(n-1) + X_0^{1-n}} \right]^{1/(n-1)} \quad (3)$$

In the particular case of  $n = 2$  and for  $X_0 = 1$ , Eq. 3 is simplified to

$$X_N = \frac{1}{1 + \kappa N} \quad (4)$$

which was first proposed by Wang and Anthony [28] to fit the marked decay of conversion shown by natural limestones along the first carbonation/calcination cycles. Yet, Eq. 4 does not account for the observed behavior at large  $N$  indicating that  $X_N$  converges towards a small residual value  $X_r$  that remains almost constant as  $N$  is further increased. Analogously, empirical studies on the deactivation of catalysts had demonstrated that  $S$  approached asymptotically to a limit or residual surface area  $S_r$  for long sintering periods. This is taken into account by the empirical general power law expression (GPLE) [25]

$$-\frac{d}{dt} \frac{S}{S_0} = k \left( \frac{S}{S_0} - \frac{S_r}{S_0} \right)^m \quad (5)$$

The GPLE equation fits well to sintering rate data on supported metal catalysts for integer values of  $m = 1, 2$  or  $3$  (first, second or third order processes, respectively) depending on the prevalent sintering mechanism. First order processes are ruled by atomic migration, while second order processes are determined by crystallite migration and agglomeration [25]. Following the parallelism with this phenomenon, the adapted version of Eq. 5 is integrated to account for the multicyclic CaO conversion behavior, which leads to

$$X_N = X_r + \left[ \frac{1}{kN(m-1) + (X_0 - X_r)^{1-m}} \right]^{1/(m-1)} \quad (6)$$

The typical decay of CaO conversion with the carbonation/calcination cycle number has been generally well fitted by the empirical equation [12]

$$X_N = X_r + \frac{1}{kN + (1 - X_r)^{-1}} \quad (7)$$

which conforms to Eq. 6 for  $X_0 = 1$  and  $m = 2$  (second order process). Experimental results obtained for most natural limestones (nonpretreated) are well fitted by Eq. 7 with values of the residual conversion  $X_r \sim 0.08$ , whereas the deactivation constant  $k$  shows a higher variability (typically between 0.5 and 2) [12]. Lysikov et al. [29] found however better regression coefficients of their fittings to experimental data by introducing a sintering exponent  $\nu$

$$X_N = X_r + \frac{1 - X_r}{(1 + kN)^\nu} \quad (8)$$

where  $\nu$  took values between 0.5 and 2. Moreover, Lysikov et al. [29] claimed that the residual CaO conversion was in fact influenced by the type of precursor and the conditions of cycling.

Underlying the approach followed to infer Eq. 6 is the assumption that the relatively soft initial CaO skeleton resulting from a quick calcination of natural limestone is prone to suffer a marked sintering along successive calcinations whereas the possible gain of surface area due to carbonation in between consecutive calcinations is neglected. The time of sintering would scale thus proportionally to the number of cycles  $t \propto N$  and the residual conversion  $X_r$  is introduced as an empirical parameter. Lysikov et al. [29] proposed an alternative view according to which CaO multicyclic conversion stabilizes at a residual value after a large number of recarbonation/decomposition cycles due to the formation of an interconnected CaO network which acts as a refractory support for an outer reactive CaO layer. A similar picture was suggested by Manovic et al. [17] to explain self-reactivation of thermally pretreated sorbents by means of a so-called pore-skeleton model. Arguably, the pore skeleton of the thermally pretreated sorbent is structured in a hard inward skeleton of low reactive CaO surrounded by a softer layer of reactive CaO with a network of small pores. The hard skeleton, developed during severe thermal pretreatment, would keep the pore structure essentially stable as the material is repeatedly subjected to carbonation/calcination cycles whereas the external soft skeleton is renovated in each recarbonation. Thus, multicyclic CaO conversion would be ruled by the balance between changes of the outward active soft skeleton during  $\text{CaCO}_3$  formation and decomposition in each calcination stage. Sintering of the external soft skeleton during the calcination phase would lead to a decrease of the surface area whereas recarbonation gives rise to an increase of the surface area by renovating the structure. In the case of limestones strongly sintered by very long isothermal preheating periods at very high temperatures, the surface area can even increase due to the prevalence of surface area gain by recarbonation to its loss by sintering, which would explain qualitatively the self-reactivation phenomenon [17].

According to Arias et al. [8, 24], self-reactivation is mainly due to the extension of carbonation beyond the fast reaction stage. This is likely to occur for severely sintered sorbents since their initial surface area and reactivity have been drastically reduced by pretreatment. This would promote reaction by solid-state diffusion, which yields after rapid decomposition a renovated porous structure with an increased reactivity and surface area

available for enhanced fast carbonation in the next cycle [8, 24]. In accordance with this view, it has been reported that conversion is significantly enhanced if the sorbent is subjected to prolonged carbonation periods (of the order of hours) even after a residual conversion is reached [22, 29]. In order to take into account the gain of activity in each cycle because of carbonation under the diffusion-controlled regime, and based on a random pore model [11], Arias et al. [8, 24] introduced an additional term  $X_{DN}$  accounting for the gain of conversion due to promoted diffusive carbonation

$$X_{DN} \approx X_N k_D \quad (9)$$

where  $k_D$  is a proportionality constant that increases with the extended carbonation time  $t_c$  according to a power law  $k_D \propto t_c^\varepsilon$  ( $\varepsilon < 1$ ) [8]. Thus, the conversion at a given cycle  $X_N$  would be determined by the balance between the conversion gain due to diffusive carbonation and the loss associated to sintering. Even though an explicit equation for conversion is not derived from this model, the algorithm detailed in ref. [8, 24] to compute conversion from this balance succeeds in predicting an increase of conversion for sufficiently large values of  $k_D$  and small values of  $X_0$  as it is the case of thermally pretreated limestones. A reasonable agreement between the calculated trend of conversion and some of the experimental data reported by Manovic et al. [17] was accomplished [24]. Further agreement with experimental data obtained by Barker [10] and Lysikov et al. [29] for prolonged carbonation periods was reported elsewhere [8]. Following the model, the conversion of a sorbent which is allowed to react under the diffusion-controlled regime would finally tend to the same apparent residual activity than the nonpretreated sorbent independently of the conditions of thermal pretreatment [24]. Yet, the model cannot explain the evolution of conversion found in some cases of activated sorbents [24]. For example, Chen et al. [22] have shown that a natural limestone and a dolomite showed a residual conversion after 1000 carbonation/calcination cycles that actually depended on the details of thermal pretreatment even though identical looping conditions are used. Furthermore, depending on the relative values of  $X_0$  and  $k_D$ , the model predicts either a continuous increase or a decrease of conversion from  $X_0$  up to reaching a residual value for large  $N$ . Yet, it is often seen that conversion of thermally pretreated sorbents increases up to reach a maximum value in a few number of cycles ( $N \lesssim 15$ ) after which  $X_N$  decreases monotonously with  $N$  [17, 19, 20].

The appendix of this manuscript shows in detail the formulation of a proposed quantita-



tive model based on the balance between the surface area gain in each cycle due to diffusive carbonation and the surface area loss due to sintering during calcination of the nascent CaO. Our experimental results (see Fig. 9 in the appendix) show that, for pretreated sorbents, there is a progressive reduction of the gain of conversion due to diffusive carbonation  $X_{Di}$  relative to the gain of conversion due to fast carbonation  $X_{Ki}$  with the cycle number  $i = 0, 1, \dots, N - 1$ . Accordingly, the relative gain of surface area is scaled with the cycle number by means of a power law equation  $S'_i/S_i = 1 + b/(i + 1)^q$ , where  $b$  is the so-called regeneration factor and the exponent  $q$  would be  $q > 0$  for thermally pretreated sorbents. On the other hand, the relative gain of conversion due to diffusive carbonation increases with the cycle number for nonpretreated sorbents ( $q < 0$ ) even though regeneration in these cases is initially small ( $b \ll 1$ ). The relative loss of surface area of the renovated soft skeleton is given by  $S_{i+1}/S'_i = 1 - a$ , where  $a$  is a so-called sintering factor related to the sintering rate  $K_s$  and sintering time  $t_s$  by means of the German-Munir model  $a = (K_s t_s)^{1/\gamma_s}$  ( $\gamma_s \simeq 2.7$  for sintering in an inert dry atmosphere) [30]. The model yields a simple analytical equation for the multicyclic CaO conversion,

$$\frac{X_N}{X_0} = (1 - a)^N (1 + b)^{N\beta} \quad (10)$$

where the so-called regeneration exponent  $\beta$  is  $\beta \simeq e^{-q}$ . In the case of thermally pretreated sorbents exhibiting self-reactivation, the regeneration factor  $b$  would be larger than the sintering factor  $a$  and it would be  $\beta < 1$ . Moreover, Eq. 10 is capable of predicting a maximum of conversion at a certain number of cycles after which it decreases monotonously with  $N$ .

The essential difference between thermally pretreated sorbents and nonpretreated ones is that, in the latter, the soft active skeleton becomes renovated due to enhanced solid-state diffusion during the first cycles whereas in the former, the initial soft active skeleton sinters progressively in each calcination without significant renovation. Although negligible in the first cycles, intermediate solid-state diffusive carbonation stages might still lead to a small gain of surface area in these cases. In order to take into account explicitly the possibility of a surface area gain in each cycle, the empirical Eq. 7 for nonpretreated sorbents, is derived in our model from a surface area gain/loss mechanism where a relative gain of surface area  $b/S_i$  is introduced (see the appendix for further details). In the case of nonpretreated sorbents (or aged pretreated sorbents after a large number of cycles at which solid-state

diffusion is already diminished), the soft active skeleton ages and loses activity in each cycle. Consequently, the relative surface area gain/loss is progressively attenuated with the cycle number. This mechanism leads to the equation

$$\frac{X_N}{X_0} = \frac{1 + b N}{1 + a N} \quad (11)$$

which is equivalent to Eq. 7 ( $a = k(1 - x_r)$ ,  $b = k x_r(1 - x_r)$ ,  $x_r = X_r/X_0$ ). In the limit  $N \gg 1$ , the ratio of gain to loss of surface area is equilibrated and conversion converges towards a residual value  $X_r = X_0 b/a$ . If attenuation of surface area gain/loss is neglected, the model leads to the equation

$$\frac{X_N}{X_0} = \frac{b}{a} + \left(1 - \frac{b}{a}\right) e^{-aN} \quad (12)$$

which conforms approximately to Eq. 10 ( $a < 1$ ) if the regeneration factor  $b$  is dismissed. Eventually, multicyclic conversion of pretreated sorbents would converge towards a residual value for very large  $N$  as seen in experimental data [22]. In this limit, Eq. 10 will no longer be suitable and the conversion evolution will be better described by Eqs. 11/12.

#### A. Analysis of multicyclic CaO conversion data for pretreated sorbents

The effect of thermal pretreatment on multicyclic CaO conversion has been extensively analyzed by Manovic and co-workers in a series of papers [17, 19, 20] as well as by other authors in the last years [18, 21–23, 29], being a subject of current debate in the literature [8, 24, 31]. The influence of preheating temperature, exposition time, type of atmosphere, type of sorbent, presence of additives, pre-hydration, pre-grinding and looping-carbonation conditions is thoroughly analyzed in these works. Let us employ the equations derived in our model to analyze the data reported in [19]. In that work benchmark looping TGA tests after pretreatment were performed isothermally at 800°C (10 min calcination and 30 min carbonation). Calcination was carried out in 100% N<sub>2</sub> while carbonation proceeded in a 50% CO<sub>2</sub> (N<sub>2</sub> balance) atmosphere. CO<sub>2</sub> concentration and time period of the looping-carbonation stage were varied in the ranges 25-100% CO<sub>2</sub> and 10-60 min, respectively, to investigate the influence of these parameters. The effect of doping a powdered limestone with  $\gamma$ -Al<sub>2</sub>O<sub>3</sub> was also analyzed. A summary of the results on multicyclic CaO conversion data reported [19] is shown in Figs. 1-3 as well as best fit curves inferred from the theory.

Multicyclic CaO conversion data for the nonpretreated powdered limestone reported in ref. [19] has been fitted by Eqs. 10, 11 and 12, which provide reasonably good fits (see Fig. 1). The best fit obtained by Eq. 10 yields  $a = 0.319$ ,  $b = 0.289$ , and  $\beta = 1.1$ . According to the model, a value of the regeneration exponent  $\beta \gtrsim 1$  indicates an increase of the relative gain of diffusive carbonation  $X_{Di}/X_{Ki}$  with the cycle number as seen in the trend of our experimental data for the nonpretreated sorbent (see Fig. 9 in the appendix). However, the best fit of Eq. 10 predicts that the conversion would start to increase when  $N$  becomes close to 30. This indicates that for this large number of cycles the relative gain of conversion due to diffusive carbonation deviates from the power law growth trend predicted by an exponent  $q = -\ln \beta < 0$  and converges towards a plateau value. Thereafter, the evolution of conversion would be better accounted for by attenuated sintering/regeneration leading to Eq. 11. Accordingly, the best fit to the data in their whole range is retrieved by using Eq. 11, which yields as best fitting parameters  $a = 0.256$  and  $b = 0.089$ . Equation 12, giving as best fitting parameters  $a = 0.210$  and  $b = 0.094$ , predicts a fast decay of conversion to a large residual value, which does not reflect the trend followed by the data. This suggests that the long-term behavior of multicyclic conversion is more properly driven by the sintering/regeneration mechanism expressed by Eqs. A25-A26 (see the appendix) for the nonpretreated sorbent.

According to the measurements reported by Borgwardt [30, 32] on the sintering of nascent CaO in an inert dry atmosphere, we may take for the sintering exponent  $\gamma_s$  a value of 2.7. Using the value of the sintering factor  $a = 0.256$  inferred and  $t_s = 10$  min (calcination time in ref. [19]), the sintering rate constant can be estimated (Eq. A3) as  $K_s = a_s^\gamma/t_s \simeq 2 \times 10^{-3}$  min<sup>-1</sup>, which is similar to the reported value by independent works [30, 33] on the sintering of nascent CaO derived from limestone in a pure  $N_2$  atmosphere at  $T = 800^\circ\text{C}$  (calcination conditions in the data reviewed [19]).

Equations 11/12 can not replicate the characteristic feature exhibited by the multicyclic conversion behavior of pretreated sorbents. In order to describe the behavior of pretreated sorbents, Eq. 10 will be thus employed. Since, according to the pore skeleton model, the soft active skeleton in pretreated sorbents will be renovated in each carbonation, its sintering during each one of the looping-calcinations will be essentially independent on the initial state. As the effect of pretreatment would be solely to enhance the gain of surface area in the diffusive carbonation stage, the sintering factor  $a$  of the soft skeleton will be kept fixed as

$a = 0.256$  in order to fit Eq. 10 to the data on the pretreated sorbents. Pretreatment would only affect the regeneration parameters  $b$  and  $\beta$  through its effect on the initial sintered skeleton to be carbonated during the subsequent cycling. A necessary requirement to hold the sintering parameter  $a$  fixed is that calcination looping conditions are not varied, which is the case under study. Using  $a = 0.256$ , Eq. 10 provides good fits to multicyclic CaO conversion data reported in ref. [19] on pretreated sorbents as may be seen in Figs. 1-3.

The best fitting parameters  $b$  and  $\beta$  to data on sorbents preheated for 24h at varying temperatures  $T$  are plotted in Fig. 4a as a function of  $T$ . In this figure, the best fit regeneration factor  $b$  previously derived for the nonpretreated sorbent is also plotted for comparison by assuming for this sorbent an equivalent preheating temperature equal to the temperature (800°C) at which carbonation/calcination looping is carried out (isothermally preheating limestone at this relatively low temperature has no appreciable influence on its conversion performance [17]). According to Fig. 4a, the parameter  $b$  grows linearly with  $T$ , which suggests that the gain of surface area in the diffusive carbonation period experienced by pretreated sorbents at these conditions increases linearly with the pretreatment temperature. On the other hand, the regeneration exponent  $\beta$  experiences a crossover from  $\beta \gtrsim 1$  to  $\beta \lesssim 1$  at  $T \simeq 1000^\circ\text{C}$ , which indicates a change around this temperature in the trend of the gain of surface area due to regeneration with the cycle number. A value of  $\beta \lesssim 1$  (for the sorbent pretreated at temperatures over around 1000°C) indicates that the gain of surface area due to diffusive carbonation decreases with the cycle number whereas it would increase with the cycle number for  $\beta \gtrsim 1$ . In the former case, the surface area after calcination of the soft pore skeleton increases with the cycle number, which causes a progressive increase of conversion but also a decrease of conversion gain during diffusive carbonation and thus a decrease of the gain of surface area with the cycle number. The opposite would happen in the latter case, i. e. there would be a decrease of the surface area after calcination and thus a decrease of conversion with the cycle number but a progressive increase of the surface area gain due to increasingly extended periods of diffusive carbonation.

The experimental results reported in [19] show that, after pretreatment at 1100°C for 6 h, the nondoped powdered limestone (Fig. 2) shows a smaller conversion as compared to the nonpretreated sorbent but self-reactivation is not achieved, i. e. CaO conversion still fades away gradually as the sorbent is cycled. For the conversion data on this nondoped powdered sorbent subjected to these mild pretreatment conditions, Eq. 11 provides a good

fit with  $b \simeq 0.283$  and  $\beta = 1.036$  (Fig. 2). As might be expected, this value of the regeneration factor is smaller than the value obtained for the powdered limestone pretreated under harsher conditions (24h at the same temperature,  $b = 0.357$ ) whereas the value of  $\beta$  is relatively larger, i.e. shortening the duration of pretreatment has a qualitatively similar effect to decreasing the pretreatment temperature.

In order to fit Eq. 10 to the data on the pretreated limestones doped with  $\gamma\text{-Al}_2\text{O}_3$  it will be assumed that the sintering rate during cyclic looping-calcination at  $800^\circ\text{C}$  is not affected notably by the small wt% of dopant ( $a = 0.256$  is kept still fixed). The trend followed by the regeneration parameters obtained with the dopant wt% (Fig. 4b) is similar to that observed with the pretreatment temperature. A higher % of  $\gamma\text{-Al}_2\text{O}_3$  helps self-reactivation by promoting sintering during preheating, which gives rise to an increment of the gain of surface area due to diffusive carbonation and to a cross over from  $\beta \gtrsim 1$  to  $\beta \lesssim 1$  (Fig. 2b).

The regeneration parameters  $b$  and  $\beta$  derived for the pretreated limestone subjected to looping-carbonation at varying  $\text{CO}_2$  % and time period ( $t_c$ ) are plotted in Figs. 4c-4d, respectively. As would be expected, the value of  $b$  is increased with the  $\text{CO}_2$  partial pressure and  $t_c$  since, in both cases, the gain of surface area during carbonation is enhanced by promoting diffusive carbonation. The crossover from  $\beta \gtrsim 1$  to  $\beta \lesssim 1$  takes place at  $t_c \simeq 20$  min while in the range of  $\text{CO}_2\%$  tested it is  $\beta \lesssim 1$ .

The trends of the regeneration factor  $b$  and the exponent  $\beta$  allow foreseeing the critical experimental conditions necessary for self-reactivation, which requires that the regeneration parameter  $b$  surmounts the sintering parameter  $a$  and that there is a crossover from  $\beta \gtrsim 1$  to  $\beta \lesssim 1$ . Harsher calcination conditions than the critical ones will increase the ratio  $b/a$  and thus the rate of increase of conversion with the cycle number but at the expenses of a smaller initial conversion  $X_0$  and a smaller value of the exponent  $\beta$ , which anticipates the maximum of conversion to a lower cycle number.

### III. EXPERIMENTAL STUDY

#### A. Materials and procedure

In our experimental study,  $\text{Ca}(\text{OH})_2$  powder from Sigma-Aldrich (purity grade puriss. p.a.) has been used as CaO precursor. Nanostructured nanosilica (Aerosil R974 from

Evonik) has been also employed in order to investigate the effect of nanosilica as a thermally stable dopant. A CaO/nanosilica composite (15% wt nanosilica) was obtained from a dry mixture of both powders (additional details on the properties of these materials and preparation method are given in ref. [34]).

Multicyclic conversion of CaO and nanosilica/CaO composite sorbents derived from preheating in-situ  $\text{Ca}(\text{OH})_2$  and  $\text{Ca}(\text{OH})_2$ /nanosilica dry mixture samples (around 10 mg) has been tested by means of TGA experiments carried out in a Q5000IR TG analyzer (TA Instruments). This equipment is provided with an infrared halogen furnace, which allows for a very fast change of temperature between cycles (up to  $500^\circ/\text{min}$  for linear heating range), and with a high sensitivity balance ( $<0.1 \mu\text{g}$ ) characterized also by a minimum baseline dynamic drift ( $<10 \mu\text{g}$ ). We highlight this point since heating rates typically employed in conventional TGA instruments (of about  $50^\circ\text{C min}^{-1}$  or even smaller [35, 36]) may give rise to nonnegligible sorbent sintering in the transitional periods, which is a source of indeterminacy to interpret the results.

Prior to carbonation/calcination cycles, the samples were preheated in-situ up to  $900^\circ\text{C}$  in either dry air or an air/ $\text{CO}_2$  mixture (85% air/15%  $\text{CO}_2$  vol/vol) according to different programs. The conventional program consisted of preheating by linearly increasing the temperature, which was performed at different rates. A novel preheating program applied (as regards the CaL analysis) was based on a technique known as Constant Rate Thermal Analysis (CRTA)[37, 38]. In the CRTA pretreatment, the evolution of temperature during preheating is controlled by means of a feedback mechanism based on mass changes during the carbonation/decarbonation reactions, which are forced to occur at prefixed low rates. The CRTA technique serves to minimize mass/heat transfer phenomena, which has been useful for obtaining materials with controlled texture and microstructure by thermally decomposing the precursors at a controlled rate [3, 39–43]. The CRTA procedure employed in our experiments maintained the carbonation/decarbonation reactions at a prefixed rate of about 0.4 %/min (weight percentage increment).

Once the material was preheated in the TG analyzer, the temperature was decreased down to at  $650^\circ\text{C}$  (cooling rate  $300^\circ\text{C}/\text{min}$ ) and the sorbent was subjected to a dry gas mixture (85% air/15%  $\text{CO}_2$  vol/vol) for carbonation to proceed during 5 minutes. In ordinary tests, the calcination stage of the cycle was carried out by heating the sorbent up to  $850^\circ\text{C}$  (heating rate  $300^\circ\text{C}/\text{min}$ ) for 5 minutes in a dry air atmosphere. Some of the tests were performed

under harsher calcination conditions (1000°C in a 10% air/90% CO<sub>2</sub> atmosphere), which are closer to those taking place in the practical application [44]. After calcination, the temperature was decreased (cooling rate 300°C/min) to proceed with the carbonation stage of a new cycle.

### B. Effect of preheating program/atmosphere and nanosilica doping

Data on the multicyclic conversion of CaO derived by preheating Ca(OH)<sub>2</sub> following diverse programs under air and air/CO<sub>2</sub> atmospheres are plotted in Fig. 5. A first look to the data reveals that preheating in air/CO<sub>2</sub> yields higher values of conversion  $X_N$ , specially in the first cycles, as compared with preheating in air. Arguably, carbonation of CaO followed by a quick decarbonation during air/CO<sub>2</sub> linear preheating program yields a relatively porous skeleton. On the other hand, a comparison of the results for the linear air/CO<sub>2</sub>-preheating programs performed at different velocities (a slow linear program at 1.5°/min taking about 440 min and a quick linear program at 20°/min taking about 40 min) shows that the preheating velocity plays a relevant influence on the trend of  $X_N$  with  $N$ . A quick preheating gives rise to a large value of conversion in the first carbonation  $X_0$  but the sorbent deactivates at a relatively higher rate indicating a relatively softer skeleton, which yields lower values of conversion at large  $N$  as compared with the slowly preheated sorbent. According to the fitting parameters obtained using Eq. 11 (table I), the effect of pretreatment by slow air/CO<sub>2</sub>-linear preheating program can be quantified by a notable increase of the regeneration factor  $b$  at the expense of a smaller  $X_0$ . This can be attributed to enhanced presintering due to the prolonged decarbonation period in a CO<sub>2</sub> enriched atmosphere. As it is widely reported in the literature [32, 45], the sintering rate of nascent CaO is accelerated in the presence of CO<sub>2</sub>, which would yield a skeleton with relatively small surface area and reactivity. Thus, diffusive carbonation in the first cycles would be promoted leading to regeneration of the skeleton in subsequent cycles.

As regards CRTA-preheating, there is not an appreciable effect as compared with the quick linear preheating program if it is performed in air (in this CRTA program the only significant reaction to be controlled is calcination of Ca(OH)<sub>2</sub>, which proceeds at around 400°C). In contrast, CRTA preheating in air/CO<sub>2</sub> produces a rather significant effect on the multicyclic conversion as can be seen in Fig. 5. To have a deep insight into this

phenomenon, there different types of CRTA programs were carried out. In the air/CO<sub>2</sub>-CRTA<sup>c</sup> mixed program, the sorbent weight gain during carbonation (starting at  $\sim 600^\circ\text{C}$ ) was kept controlled at a very small rate for about 60 min to complete carbonation, after which the temperature was increased up to  $900^\circ\text{C}$  following a quick linear program (at  $20^\circ\text{C}/\text{min}$ ), which makes decarbonation (starting at about  $800^\circ\text{C}$ ) to occur at a fast and uncontrolled rate. For this mixed CRTA-Linear program, the initial conversion  $X_0$  is very large (close to one) as seen in Fig. 5, which suggests that the sorbent structure that results after preheating is highly porous. A controlled and slow carbonation of the sorbent during a long time period favors solid-state diffusion of CO<sub>2</sub>, which would yield after fast decarbonation a highly porous sorbent with a large surface area and reactivity in the first cycle. Yet, it is seen in Fig. 5 that  $X_N$  decreases at a high rate as the sorbent is further cycled over. This indicates a marked sintering of this initially porous and soft skeleton when subjected to looping-calcination whereas regeneration during carbonation in the diffusive phase of the cycles is negligible. Interestingly, the opposite trend is obtained if CRTA pretreatment in air/CO<sub>2</sub> is operated by controlling both carbonation and decarbonation reactions to keep them at a small prefixed rate. Under this full CRTA program, (slow and controlled) carbonation takes place in about 60 min and (slow and controlled decarbonation) lasts about 120 min. After preheating the sorbent under this program,  $X_0$  is rather small as the resulting skeleton would have suffered appreciable sintering during prolonged slow decarbonation in a CO<sub>2</sub> enriched atmosphere. However, as the number of cycles is increased, CaO conversion diminishes slowly with the cycle number and relatively large values of conversion are preserved after a large number of cycles. Thus, in the air/CO<sub>2</sub>-CRTA preheating program, the highly presintered sorbent by slow decarbonation would significantly gain surface area due to diffusive carbonation in the first cycles. Finally, if a mixed Linear-CRTA preheating program is carried out in air/CO<sub>2</sub> by initially increasing the temperature in the quick linear preheating program for carbonation to proceed fast but keeping subsequent decarbonation at a small controlled rate (air/CO<sub>2</sub>-CRTA<sup>d</sup> preheating program),  $X_0$  is further decreased (see Fig. 5). In this mixed program, the surface area of the preheated sorbent would be very small since diffusive carbonation during preheating is hindered because of quick carbonation. On the other hand, sintering is enhanced during slow and controlled CRTA decarbonation in air/CO<sub>2</sub>. As a consequence, the preheated skeleton would become highly sintered with very small surface area and reactivity. SEM micrographs and BET surface area measurements of samples pretreated in air/CO<sub>2</sub>



under the linear and CRTA<sup>d</sup> preheating programs support these arguments. As can be seen in Fig. 7, the CRTA preheated sorbent (BET=3.87 m<sup>2</sup>/g) exhibits a higher level of sintering with larger pores as compared with the linearly preheated sorbent (BET=9.04 m<sup>2</sup>/g).

In Fig. 6, CaO conversion data have been plotted for the CaO/nanosilica composite subjected to air-linear and air/CO<sub>2</sub>-CRTA preheating programs as well as data corresponding to CaO previously analyzed for comparison. The most notable effect of nanosilica is to increase the first cycle conversion  $X_0$  in any of the preheating programs. This effect may be rationalized from a thermal stabilization of the CaO skeleton during preheating and the improvement of CaO dispersibility, which helps to expose small pores of the CaO skeleton for fast CO<sub>2</sub> sorption [34]. In spite of the relatively higher value of  $X_0$ , the multicyclic conversion decay of the linear preheated CaO/nanosilica composite does not suffer an appreciably strong decay with the cycle number as compared to CaO since nanosilica would also prevent sintering during looping-calcination. The beneficial effect of doping with silica on preventing sintering of CaO sorbents is reported also in diverse works in the literature [46–48].

Concerning the multicyclic conversion of the air/CO<sub>2</sub> preheated sorbents, the best fit of Eq. 10 to the 50 cycles data gives values of the regeneration exponent  $\beta \gtrsim 1$  as it is the typical feature of thermally pretreated sorbents not showing self-activation. However, a closer look into the first 5-10 cycles reveals that conversion data in this region deviates from the curve drawn from the best fit of Eq. 10 to the 50 cycles data. A zoom of the data for air/CO<sub>2</sub>-CRTA preheated CaO and CaO/nanosilica (inset of Fig. 6) evidences instead a slight augmentation of conversion in the 2nd cycle followed by a very slow decrease of it in the next cycles. Accordingly, the best fit of Eq. 10 to only data on the first 6 cycles (dashed curve in Fig. 6) yields a value of the regeneration exponent  $\beta \lesssim 1$  and of the regeneration factor  $b$  larger than the sintering factor  $a$  (table I). Note in the inset of Fig. 6 that for the (air/CO<sub>2</sub>-CRTA preheated) CaO/nanosilica composite, conversion decays at a faster rate with  $N$  than for CaO. As nanosilica hampers sintering during preheating, the initial skeleton would be softer, which would give a smaller ratio of regeneration to sintering factor  $b/a$  (1.189 for CaO/nanosilica vs. 1.383 for CaO). In this regard, the effect of nanosilica would be opposed to that of  $\gamma$ -Alumina observed in [19], which promoted sintering during pretreatment. After about 20 cycles the data trend for the CaO/nanosilica composite adjusts to a similar rate of decay than for CaO. Short-term self-activation may be identified also

for the pretreated sorbent at the lowest temperature (1000°C) in the data shown in Fig. 1.

CaO from preheating Ca(OH) <sub>2</sub>				
↓ Preheating program	$a$	$b$	$\beta$	Eq.
Linear (air/CO <sub>2</sub> ) quick	0.164	0.024	1	11
Linear (air/CO <sub>2</sub> ) slow	0.164	0.123	1.083	10
Linear (air) quick	0.145	0.042	1	11
CRTA (air)	0.145	0.032	1	11
CRTA <sup>c</sup> (air/CO <sub>2</sub> )	0.266	0.042	1	11
CRTA (air/CO <sub>2</sub> )	0.266/0.266	0.348/0.368	1.001/0.980	10/10( $N \leq 5$ )
CRTA <sup>d</sup> (air/CO <sub>2</sub> )	0.266	0.325	1.01	10

CaO/nanosilica from preheating Ca(OH) <sub>2</sub> /nanosilica				
↓ Preheating program	$a$	$b$	$\beta$	Eq.
Linear (air) quick	0.186	0.061	1	11
CRTA (air/CO <sub>2</sub> )	0.186/0.186	0.191/0.221	1.03/0.957	10/10( $N \leq 5$ )

Harsh looping calcinations					
↓ Sorbent	$a$	$\alpha$	$b$	$\beta$	Eq.
CaO	0.508/0.478	1/0.345	0.063/0.0012	1/1	11/17
CaO/nanosilica	0.693/0.410	1/0.423	0.087/0.0018	1/1	11/17

TABLE I. Sintering and regeneration parameters obtained from the fitting of Eqs. 10/11/17 to experimental data on the CaL multicyclic conversion of CaO and CaO/nanosilica derived from Ca(OH)<sub>2</sub> and Ca(OH)<sub>2</sub>/nanosilica mixtures preheated under different programs as indicated. For tests applying harsh looping calcination conditions (1000°C and 90%CO<sub>2</sub> vol) the preheating program consisted of a quick linear preheating program in air/CO<sub>2</sub> (90%CO<sub>2</sub> vol).

### C. Effect of harsh looping calcination conditions

Multicyclic CaO conversion data obtained when the sorbents are subjected to harsh looping-calcination conditions (90% vol CO<sub>2</sub> atmosphere at 1000°C) are plotted in Fig. 8.

In this figure, data on conversion taken just at the end of the fast carbonation phase ( $X_{KN}$ ) have been also drawn. Under harsh looping-calcination conditions the sorbent suffers a severe sintering, and the consequent drastic loss of surface area and reactivity yields a very small conversion in the fast phase. As seen in Fig. 9 (appendix), the ratio of conversion gain in the diffusive carbonation period ( $X_{DN}$ ) to conversion in fast carbonation ( $X_{KN} = X_N - X_{DN}$ ) is larger than unity, i.e. a significant part of the total conversion measured at the end of the carbonation stage is due to diffusive carbonation in spite that carbonation was maintained for only 5 min. Even though diffusive looping-carbonation is relatively large, sintering of the skeleton during looping-calcination fairly prevails on regeneration at these harsh looping-calcination conditions. Accordingly, the best fit of Eq. 11 to the data gives rise to very large values of the sintering factor  $a$  as compared with the regeneration factor  $b$  (see table I), which leads to a rapid convergence of conversion towards a small residual value. However, as it is appreciated in Fig. 8 (see the inset), the best fits curves from Eq. 11 do not adjust satisfactorily to the data in the first cycles.

The sintering rate of nascent CaO, as determined by BET surface area measurements [30, 32, 45], is greatly accelerated by the increase of CO<sub>2</sub> partial pressure  $P_{CO_2}$  and temperature  $T$ . From an extensive review of the results published in the literature, Stanmore and Gilot [32] have concluded that the German-Munir equation (Eq. A1) is the most flexible and reliable model to interpret the majority of the data reported, yet it can be justified only for  $a = \Delta S/S_0 = (K_s t_s)^{1/\gamma_s} < 0.5$ . For sintering of CaO in pure N<sub>2</sub> [30], it is  $\gamma_s \simeq 2.7$  and, for nascent CaO derived from limestone,  $K_s \simeq 2 \times 10^{-3} \text{ min}^{-1}$  at  $T = 850^\circ\text{C}$  (mild calcination conditions in our experiments). Accordingly, it would be  $a = (K_s t_s)^{(1/\gamma_s)} \simeq 0.18$  for  $t_s = 5$  min (looping-calcination time period in our experiments), which fits in the validity range of the German-Munir model. Note that this value of  $a$  is very close to the value obtained from the fit of Eqs. 10-12 to our conversion data on CaO subjected to mild looping-calcination conditions (table I). Sintering in a CO<sub>2</sub> enriched atmosphere changes the driving force from a lattice diffusion mechanism to a catalytic mechanism, which yields much larger values of the sintering exponent  $\gamma_s$ . A review of experimental data reported in the literature shows that the functional dependence of the sintering rate constant  $K_s$  and of  $\gamma_s$  on  $T(^{\circ}\text{K})$  and  $P_{CO_2}(\text{Pa})$  can be expressed as [32]

$$\ln K_s = 18.5 + 0.558 \ln P_{CO_2} - \frac{30000}{T} \quad (13)$$

$$\gamma_s = 44.1(0.8 \ln P_{CO_2} - 1) \exp\left(-\frac{4140}{T}\right) \quad (14)$$

Empirical correlations given by Eqs. 13-14 are based on fittings made by Stanmore and Gilot [32] to raw data published by Borgwardt [45] (misprints in the original fitting equations reported in [45] are noted). Data are available from measurements performed at temperatures up to 1150°C and CO<sub>2</sub> pressures up to 18.2 kPa. If we assume that Eqs. 13-14 can be extrapolated to higher CO<sub>2</sub> pressures we may use them to estimate values of  $K_s = 3.67 \text{ min}^{-1}$  and  $\gamma_s = 13.87$  in the case of our harsh looping-calcination conditions ( $T = 1000^\circ\text{C}$  and  $P_{CO_2} = 90 \text{ kPa}$ ), which would lead to a value of  $a = 1.1$  that clearly oversteps the range of applicability of the German-Munir model.

It is therefore explainable that Eq. 11 fails to provide a fully satisfactory fit to conversion data measured under harsh looping-calcination conditions as seen in Fig. 8. In this limit, it is likely that sintering in each calcination provokes a drastic decrease of surface area, which might attain values not far from its residual value  $S_r$ . Thus, it would be more appropriate to use the GPLE equation (Eq. 5) to describe the surface area loss in looping-calcination, which has been successfully used to interpret data on strong sintering of nascent CaO with  $m = 2$  [49]. Integration of Eq. 5 yields

$$\frac{S - S_0}{S_0} = -kt_s \frac{(S_0 - S_r)(S - S_r)}{S_0^2} \quad (15)$$

The adapted form of Eq. 15, for the purpose of our multicyclic conversion model, to calcination in the  $i$ th cycle conforms to

$$\frac{S_{i+1}}{S'_i} = 1 - kt_s \sigma(i) \quad (16)$$

with  $\sigma(i) = (S'_i - S_r)(S_{i+1} - S_r)/(S'_i)^2$ . Equation 16 reflects the fact that the sintering factor  $a(i) = kt_s \sigma(i)$  becomes now a function of the cycle number. For severe sintering, the surface area after the calcination stage  $S_{i+1}$  and the surface area after carbonation  $S'_i$  will approach the residual value  $S_r$  at a higher rate as the cycle number is increased. Thus, it seems reasonable to assume  $\sigma(i) = \sigma/(i+1)^p$  where  $\sigma \ll 1$  and  $p > 0$  is an exponent that depends on the harshness of the looping-calcination conditions. Proceeding analogously as in

the derivation of 10 (see the appendix), a more general equation for describing the evolution of multicyclic CaO conversion would be

$$\frac{X_N}{X_0} = (1 - a)^{N^\alpha} (1 + b)^{N^\beta} \quad (17)$$

where the sintering factor is  $a = kt_s\sigma$ . The sintering exponent  $\alpha$  is  $\alpha \approx e^{-p} < 1$ , being closer to one the less severe looping-calcination conditions are.

Equation 17 should serve to fit more accurately our multicyclic conversion data for harsh looping-calcination conditions. In order to reduce the number of free parameters, we will consider  $\beta \approx 1$  since for severe looping-calcination the regeneration factor will be outweighed by the sintering factor ( $b \ll a$ ) and thus there will be little influence of the actual value of the exponent  $\beta$ . As may be checked in Fig. 8 the best fit curve from Eq. 17 (with  $\beta = 1$ ) adjusts well to conversion data on both CaO and CaO/nanosilica sorbents with  $b \ll a$  as expected (table I). As regards the effect of nanosilica doping, it is seen that it yields a smaller value of  $a$ , indicating that it lessens sintering, whereas it gives a larger value of  $b$  as it would help to increase the gain of activity due to diffusive carbonation. From the fitting values of  $\alpha$ , the estimated value of the exponent  $p \approx -\ln \alpha$  is smaller for the CaO/nanosilica composite ( $p \approx 0.861$ ) than for CaO ( $p \approx 1.065$ ) implying that nanosilica slows down the approach of the surface area to its residual value by preventing sintering. Typical values reported for the sintering rate constant  $k$ , derived in the literature from fitting measurements on the sintering of CaO to Eq. 5 [32, 49], are  $k \sim 1 \text{ s}^{-1}$  for  $T \simeq 1000^\circ\text{C}$ . Using  $a = kt_s\sigma \simeq 0.4$  from the fitting of Eq. 17 to our data (table I) and  $t_s = 300 \text{ s}$  (calcination time in our experiments), it would be  $\sigma \sim 10^{-3}$ , in agreement with the hypothesis made to derive Eq. 17 ( $\sigma \ll 1$ ).

#### IV. CONCLUSIONS

In this work we have analyzed the conversion behavior of CaO subjected to a series of repeated carbonation/calcination cycles. An analytical equation is derived from a model based on the balance of surface area gain/loss experienced by the sorbent during carbonation/calcination. This equation has been satisfactorily fitted to data on the evolution of multicyclic CaO conversion as influenced by a diversity of experimental variables such as preheating program, atmosphere composition, presence of additives and carbona-

tion/calcination conditions. In the light of the proposed model, the conversion behavior exhibited by pretreated sorbents has been quantified in terms of the values of regeneration and sintering factors ( $b$  and  $a$ , respectively) and a regeneration exponent  $\beta$ . Whereas  $b$  and  $\beta$  determine the evolution of the gain of surface area due to solid-state diffusive carbonation as the sorbent is cycled over,  $a$  determines the loss of surface area due to sintering in the looping-calcination stage. In all the cases examined showing self-reactivation (increase of CaO conversion with the cycle number), the regeneration factor  $b$ , which according to a generalized (second order) power law expression (GPLe) is proportional to the extended carbonation time  $t_c$ , turns to be larger than the sintering factor  $a$ , which scales as  $(K_s t_s)^{1/\gamma_s}$ , being  $t_s$  the sintering time and  $\gamma_s \simeq 2.7$  according to the German-Munir model. The values of  $a$  derived from the fittings to experimental data yield estimated values of the sintering rate constants  $K_s$  similar to the one obtained from independent measurements of the BET surface area of nascent CaO. The results indicate that self-reactivation ( $b > a$ ) is accompanied by a cross-over of the regeneration exponent  $\beta$  from  $\beta \gtrsim 1$  to  $\beta \lesssim 1$ . For  $\beta \gtrsim 1$ , which is characteristic of nonpretreated sorbents, the relative gain of conversion in the diffusive carbonation phase increases with the cycle number. For thermally pretreated sorbents showing self-reactivation ( $\beta \lesssim 1$ ), it decreases with the cycle number.

The harsher the pretreatment conditions are (higher temperature and longer exposition periods) the more sintered the initial skeleton becomes, which gives rise to an initial hard skeleton with very small surface area and reactivity where diffusive carbonation is promoted ( $b > a$ ). An active soft skeleton is regenerated during promoted solid-state diffusive carbonation. After quick decarbonation, the surface area and reactivity increases for the next carbonation provided that sintering of nascent CaO during looping-calcination is not significant. The relative gain of conversion due to diffusive carbonation with the cycle number is progressively reduced and eventually conversion reaches a maximum value. As regards nonpretreated sorbents, there is a growth of diffusive carbonation with the cycle number due to the gradual sintering of the initial soft skeleton and the consequent decrease of the surface area available for fast carbonation. Even though regeneration in nonpretreated sorbents is small in the first cycles, it grows as the number of cycles is increased until the surface area loss is equilibrated by the surface area gain and a residual conversion is reached.

Experiments reported in this manuscript on CaO and CaO/nanosilica composite sorbents derived from preheating  $\text{Ca(OH)}_2$  and  $\text{Ca(OH)}_2/\text{nanosilica}$  dry mixtures according to

diverse programs have served to shed further light on the mechanism responsible for either enhancing or hindering multicyclic CaO conversion. Of particular interest have been the results obtained from a preheating CRTA program in which a feedback mechanism controls the temperature to keep the carbonation/decarbonation rates at a prefixed constant and small value. By carrying out this preheating program in an air/CO<sub>2</sub> atmosphere it has been seen that a rapid carbonation of the sorbent followed by a slow and prolonged decarbonation gives rise to a highly sintered structure yielding a small CaO conversion in the first cycle, self-reactivation in the first cycles and slow conversion decay afterwards. On the other hand, carbonation of the sorbent at a slow rate during a prolonged period of time followed by fast decarbonation gives rise to a large value of conversion in the first cycle that decays drastically with the cycle number. In this case slow and controlled carbonation during preheating promotes CO<sub>2</sub> solid-state diffusion, which results in a highly porous soft skeleton after fast decarbonation.

In our experimental work we have further analyzed the multicyclic behavior of sorbents subjected to harsh looping-calcination conditions. Under these circumstances, sintering during the looping-calcination stages is more appropriately modeled by using a second order GPLE equation yields, which yields a modified surface area loss equation to describe the evolution of conversion. Experimental results obtained on CaO and CaO/nanosilica composite sorbents show that nanosilica prevents sintering thus enhancing fast carbonation. In the case of harsh looping-calcination conditions, fast carbonation is severely constrained and the presence of nanosilica serves also to enhance diffusive carbonation.

## V. ACKNOWLEDGEMENTS

This work was supported by the Andalusian Regional Government (Junta de Andalucía, contract FQM-5735) and Spanish Government Agency Ministerio de Ciencia e Innovación (contracts FIS2011-25161 and CTQ2011-27626). The collaboration of Dr. C. Soria-Hoyo in the analysis of the experimental results is warmly appreciated.

## Appendix A: Models on the multicyclic CaO conversion behavior

### 1. Thermally pretreated sorbents

A theoretical model which has been successfully used to interpret experimental results on the surface area loss of nascent CaO [30, 32, 33, 45, 50] (and other types of materials [26, 51, 52]) when subjected to short-timed isothermal heating is the German-Munir model [26]. The model is grounded on the assumption that the initial decrease of CaO surface area is driven by the curvature gradient in the neck region between contacting grains, which leads to the simple equation

$$\left(\frac{S_0 - S}{S_0}\right)^{\gamma_s} = K_s t_s \quad (\text{A1})$$

where  $t_s$  is the sintering time,  $K_s$  is the sintering rate constant, which is a function of the diffusion coefficient and surface tension, and increases with temperature  $T$  according to an Arrhenius relationship, and  $\gamma_s$  is a characteristic exponent, which depends on the predominant mass transport mechanism [30]. An extensive series of measurements on the sintering rate of nascent CaO indicated that the sintering exponent takes a value essentially independent of  $T$  and precursor type of  $2.7 \pm 0.3$ , which is consistent with the mechanism of lattice diffusion. The sintering rate  $K_s$  depends on the type of precursor and presence of impurities [30]. Defects in the crystal lattice enhances lattice diffusion while lower porosity implies closer contact between grains and thus a greater propensity for neck formation [32]. On the other hand, the sintering rate at a given temperature was observed to be greatly increased by the presence of  $H_2O$  and  $CO_2$  [33, 45].

The neck-growth model used to infer Eq. A1 is strictly valid only for  $(S_0 - S)/S_0 < 0.5$ . As sintering progresses, a shift in the dominant driving force from the neck curvature gradient (described by Eq. A1) to surface energy minimization (described by Eq. 1) takes place [26]. Let us consider the sintering suffered by nascent CaO (from the soft skeleton formed due to diffusive carbonation) during the looping-calcination stage of the  $i$ th cycle. Since the sintering period in this stage is small (typically of a few minutes), and nascent CaO derives from a just renovated soft skeleton, Eq. A1 can be judged as the most appropriate to estimate the surface area at the end of  $i$ th calcination ( $S_{i+1}$ ),



$$\frac{S_{i+1}}{S'_i} = 1 - a \quad (i = 0, 1, \dots, N - 1) \quad (\text{A2})$$

where

$$a = (K_s t_s)^{1/\gamma_s} \quad (\text{A3})$$

$t_s$  is the calcination time and  $S'_i$  is the surface area of nascent CaO just after the  $i$ th decarbonation. It will be  $S'_i > S_i$  since the pore skeleton will be regenerated due solid-state diffusion mechanism and the subsequent release of CO<sub>2</sub> taking place immediately before sintering. To incorporate into the model the gain of surface area due to diffusive carbonation, the simplest choice would be to use a German-Munir equation type where the sintering rate constant is replaced by a regeneration rate constant. However, this equation might be appropriate only if the relative gain of surface area is small whereas it can be otherwise for thermally pretreated sorbents. In this case, it is likely that the rate of surface area gain decreases as it approaches a maximum value  $S_c$ . Then, it would be more suitable to use an adaptation of the GPLE equation (Eq. 5),

$$+\frac{d}{dt} \frac{S}{S_0} = k_c \left( \frac{S - S_c}{S_0} \right)^2 \quad (\text{A4})$$

where a regeneration rate constant  $k_c$  is introduced and it has been assumed  $m = 2$ . By integration of Eq. A4 we arrive at

$$\frac{S}{S_0} = 1 + k_c t_c \frac{(S_0 - S_c)(S - S_c)}{S_0^2} \quad (\text{A5})$$

where  $t_c$  is the extended carbonation time. Equation A5 adapted to carbonation in the  $i$ th cycle ( $S = S'_i, S_0 = S_i$ ) is written as

$$\frac{S'_i}{S_i} = 1 + k_c t_c \frac{(S_i - S_c)(S'_i - S_c)}{S_i^2} = 1 + k_c t_c \delta(i) \quad (i = 0, 1, \dots, N - 1) \quad (\text{A6})$$

In Eq. A6  $\delta(i) \equiv (S_i - S_c)(S'_i - S_c)/S_i^2$  would depend on the cycle number  $i$  since, generally, the gain of surface area might vary as the cycle number is increased. For  $\delta(i) = \text{constant}$ , Eq. A6 is reminiscent of Eq. 9 which was proposed by Grasa et al. [11] to account for the additional gain of activity ( $X_{Di}$ ) due to solid-state diffusion carbonation. This simple lineal relationship was justified from the approximate trend followed by experimental data on the

multicyclic conversion of a nonpretreated limestone [11] showing a relative gain of activity in the diffusive phase  $X_{Di}/X_{Ki}$  that would be independent of the cycle number  $i$ . Yet, and since  $k_D$  would be a function of the diffusive carbonation time ( $k_D \propto t_c^\varepsilon$ ), it might vary as a function of the cycle number if  $t_c$  changes. For example, if the active skeleton loses surface area with the cycle number, the fast carbonation period will be shortened. Being the total carbonation period fixed, the diffusive carbonation period will be gradually lengthened in subsequent cycles. In this case  $\delta(i)$  in Eq. A6 ( $k_D$  in Eq. 9) would grow with the cycle number.

The evolution of  $X_{Di}/X_{Ki}$  may show a variable behavior depending on the type of sorbent, thermal pretreatment and conditions of looping carbonation/calcination. This is clearly seen in Fig. 9, where  $X_{Di}/X_{Ki}$  is plotted as a function of  $i$  for the CaO and CaO/nanosilica sorbents analyzed in our experimental work and subjected to diverse preheating programs. As can be observed,  $X_{Di}/X_{Ki}$  converges towards a constant value in all the cases at large  $i$ . Yet,  $X_{Di}/X_{Ki}$  may exhibit a marked variation along the first cycles depending on the experimental conditions. In the case of CaO derived from the air/CO<sub>2</sub>-CRTA preheating program,  $X_{Di}/X_{Ki}$  reaches a constant value ( $\approx 0.8-0.9$ ) just after 3-4 cycles. However, Fig. 9 shows also that in the case of CaO obtained from the quick linear preheating program,  $X_{Di}/X_{Ki}$  is small for the first carbonation ( $\approx 0.2$ ) but it increases with the cycle number to converge for  $i \gtrsim 50$  towards the same value that for the air/CO<sub>2</sub>-CRTA preheated CaO. A straightforward qualitative explanation for this behavior would be that the soft skeleton of the quickly preheated sorbent is prone to be gradually sintered along successive looping-calcinations. Thus, the surface area available for fast sorption becomes progressively reduced, which leads to an increase of the relative gain of conversion in the diffusive phase of the fixed carbonation period (5 min). The progressive increase of  $X_{Di}/X_{Ki}$  continues until the skeleton is sufficiently hardened after about 50 carbonation/calcination cycles. Interestingly, this observation suggests that the main effect of thermal pretreatment by CRTA is to anticipate to the first cycles the aging that the skeleton of the quickly preheated sorbent suffers only after a large number of repeated calcinations. A further remarkable feature illustrated by Fig. 9 is that if CaO is doped with nanosilica,  $X_{Di}/X_{Ki}$  increases from a similar initial value than for the nondoped sorbent ( $\approx 0.2$ ) to a plateau value  $\approx 0.4$  (less than half of the value corresponding to the nondoped sorbent at large  $i$ ) after just about 10 cycles. Since nanosilica provides the sorbent with improved thermal stability [34], sintering induced by

looping-calcination is hindered, which favors fast carbonation against diffusion. Remarkably, a similar quick convergence towards a plateau value is observed for both the sorbent doped with nanosilica and the one thermally stabilized by air/CO<sub>2</sub>-CRTA preheating, even though the  $X_{Di}/X_{Ki}$  plateau value is smaller in the former case. In this regard, the stabilizing effect of the additive would be potentially more advantageous since sorption would be mainly enhanced in its kinetic fast phase of interest from practical applications. In all the cases examined in Fig. 9 up to now it is  $X_{Di}/X_{Ki} < 1$ . Since looping-calcination conditions are not harsh (850°C in air), there is not a drastic reduction of surface area during each calcination, which allows for a relatively large conversion in the fast carbonation phase. However, if the sorbent is subjected to harsher looping-calcination conditions (1000°C in a 90% CO<sub>2</sub>/10% air atmosphere), diffusive carbonation is promoted against fast carbonation ( $X_{Di}/X_{Ki} > 1$ ) due to the strong sintering induced by calcination at very high temperature and CO<sub>2</sub> concentration [45]. This causes a marked decrease of the surface area available and promotes diffusive carbonation. Under these harsh looping-calcination conditions, doping with nanosilica serves to further enhance diffusive carbonation.

These results clearly show that although  $X_{Di}/X_{Ki}$  converges eventually towards a constant value, even though its variation along the first cycles might play a relevant role in the evolution of the multicyclic conversion. Accordingly, in Eq. A6 it will be assumed  $\delta(i) = \delta/(i+1)^q$ , where  $q$  is a parameter whose value will depend on the type of sorbent and on experimental conditions, and  $\delta$  is a constant. As inferred from the suitability of a power law fit to our experimental data on the relative gain of diffusive conversion (Fig. 9) this dependence seems to be justified at least for the first cycles. Note in Fig. 9 that a particular feature of the evolution of  $X_{Di}/X_{Ki}$  for the air/CO<sub>2</sub>-CRTA preheated sorbent is that it actually decreases along the very first cycles. This implies that decarbonation in these first cycles gives rise to a higher surface area than in the previous cycle, which allows for relatively longer fast carbonation periods as compared with the precedent cycle and thus to shorter diffusive carbonation periods. Thus, in the case of our CRTA pretreated sorbents,  $\delta(i)$  would be a decreasing function of  $i$  ( $q > 0$ ) whereas for the quickly preheated sorbent  $\delta(i)$  should increase with  $i$  ( $q < 0$ ). Thus,

$$\frac{S'_i}{S_i} = 1 + k_c t_c \frac{\delta}{(i+1)^q} \quad (i = 0, 1, \dots, N-1) \quad (\text{A7})$$

From a Taylor series expansion ( $\delta < 1$ ) it is

$$1 + k_c t_c \frac{\delta}{(i+1)^q} \simeq (1 + \delta)^{\frac{k_c t_c}{(i+1)^q}} - \frac{k_c t_c}{2(i+1)^{2q}} \left( \frac{1 - (i+1)^q}{(i+1)^q} \right) \delta^2 \quad (\text{A8})$$

Since the second term in the right hand side of Eq. A8 will be negligible, it can be written

$$\frac{S'_i}{S_i} \simeq (1 + \delta)^{\frac{k_c t_c}{(i+1)^q}} \quad (i = 0, 1, \dots, N-1) \quad (\text{A9})$$

Assuming  $X \propto S$ , we can write

$$\frac{X_N}{X_0} \simeq \frac{S_N}{S_0} = \prod_{i=0}^{N-1} \frac{S_{i+1}}{S_i} = \prod_{i=0}^{N-1} \frac{S_{i+1}}{S'_i} \cdot \frac{S'_i}{S_i} \quad (\text{A10})$$

which, using Eqs. A2-A9, leads to

$$\frac{X_N}{X_0} \simeq (1-a)^N \prod_{i=1}^N (1 + \delta)^{\frac{k_c t_c}{i^q}} = (1-a)^N (1 + \delta)^{k_c t_c \sum_{i=1}^N \frac{1}{i^q}} = (1-a)^N (1 + \delta)^{k_c t_c H(N,q)} \quad (\text{A11})$$

where  $H(N, q) = \sum_{i=1}^N \frac{1}{i^q}$  is a special function so-called Harmonic-Number function. It is possible to find an approximate analytical expression for this special function by calculating the discrete summation as the integral of a continuous function,

$$H(N, q) = \sum_{i=1}^N \frac{1}{i^q} \approx \int_0^N \frac{dx}{(x + \frac{1}{2})^q} = \frac{1}{1-q} \left[ \left( N + \frac{1}{2} \right)^{1-q} - \left( \frac{1}{2} \right)^{1-q} \right] \quad (\text{A12})$$

Alternatively, this function may be fitted to power law by a least squares fit,  $H(N, q) \simeq N^\beta$  with  $q \approx -\ln \beta$  (see Fig. 10). In the limit  $\beta = 1$  ( $q = 0$ ), it is  $H(N, 0) = N$ .

Summarizing, the model yields a compact analytical equation for the evolution of the CaO conversion with the cycle number,

$$\frac{X_N}{X_0} = (1-a)^N (1+b)^{N^\beta} \quad (\text{A13})$$

where  $b = k_c t_c \delta$  is a so-called regeneration factor and it has been used  $(1 + \delta)^{k_c t_c} \simeq 1 + k_c t_c \delta$  for  $\delta < 1$ .

In the case of thermally pretreated sorbents, the regeneration factor  $b$  could be relatively large, in fact larger than the sintering factor  $a$ . Generally, Eq. 10 may describe the diversity of behaviors observed for pretreated sorbents in the first cycles [17–22] depending on the relative values of  $a$ ,  $b$  and  $\beta$  such as the presence of a maximum of conversion at a certain

value of  $N$ . This maximum will exist in the case  $b > a$  and  $\beta < 1$  and will be placed at a cycle number  $N_0$

$$N_0 = \left[ \frac{\beta \log(1+b)}{-\log(1-a)} \right]^{1/(1-\beta)} \quad (\text{A14})$$

which, for given values of  $b$  and  $a$ , is larger the closer  $\beta$  becomes to unity (the surface area gain associated with diffusive carbonation decreases at a slower rate with the cycle number). Small values of  $\beta$  would yield self-reactivation just for a reduced number of cycles (that would be the case of the air/CO<sub>2</sub> preheated sorbent in our experiments) after which conversion would decrease at a slow rate. Thus, a slight deviation of the exponent  $\beta$  from unity (or equivalently of the exponent  $q$  around zero) can be of importance to determine the evolution of conversion for pretreated sorbents. If  $b < a$ , the surface area loss will rule over surface area gain and conversion will decrease initially even though it is  $\beta > 1$ .

## 2. Nonpretreated sorbents

In the cases of nonpretreated sorbents there will be an increase of the surface area gain due to diffusive carbonation (as indicated by data in Fig. 9) with the cycle number (in terms of Eq. A13 it would be  $\beta > 1$ ) even though conversion decreases markedly with the cycle number as sintering prevails on regeneration ( $b \ll a$ ). If regeneration were fully neglected as compared to sintering in Eq. A13 ( $b = 0$ ), an equation is retrieved,

$$\frac{X_N}{X_0} = (1-a)^N \quad (\text{A15})$$

which would take into account only a continuous loss of surface area at a constant rate in each cycle. Equation A15 has been already proposed in the work of Wang and Anthony [28] but it predicts a too drastic rate of decay of conversion that does not fit well to long-series of multicyclic conversion data on nonpretreated sorbents. A similar empirical equation had been earlier proposed by Abanades [53] ( $X_N/X_0 = f^N + g$ ), that was later [54] modified to

$$\frac{X_N}{X_0} = f_m^N (1 - f_w) + f_w \quad (\text{A16})$$

which was justified by the addition to the conversion associated with microporosity ( $X_{Nm} = f_m^N X_0$ ) a further contribution due to the increase of large pores produced by the loss of

microporosity (assumed to be  $X_w = f_w(1 - X_{Nm})$ ). Equation A16 was reported to reasonably fit short-series of multicyclic conversion data on nonpretreated sorbents [54].

It may be argued that the German-Munir model for sintering might be applicable to analyze the conversion behavior of nonpretreated sorbents for a small number of cycles. However, and since the behavior of these sorbents would be mainly determined by the sintering of an initial soft pore skeleton without significant renovation in the carbonation stages, the rate of sintering of this progressively aged skeleton should decrease significantly as the number of cycles builds up. By assuming that the sintering factor decreases in each cycle proportionally to the surface area and that there is not regeneration, the surface area gain/loss balance equations would be

$$\frac{s_{i+1}}{s_i} = 1 - a s_i \quad (\text{A17})$$

$$\frac{s'_i}{s_i} = 1 \quad (\text{A18})$$

$$s_N - 1 = \sum_{i=0}^{N-1} s_{i+1} - s_i = -a \sum_{i=0}^{N-1} s_i^2 \quad (\text{A19})$$

where it is defined  $s_i = S_i/S_0 = X_i/X_0$  and it has been made explicit that regeneration in the diffusive carbonation period is neglected ( $s'_i = s_i$ ). This summation is easily carried out by adopting a continuum analysis. The differential form of Eq. A17 ( $ds = -as^2 di$ ) becomes then analogous to the empirical rate equation (Eq. 1), leading by integration to

$$\frac{X_N}{X_0} = \frac{1}{1 + a N} \quad (\text{A20})$$

which is equivalent to Eq. 4, firstly derived by Wang and Anthony [28]. As it has been reported in the literature, Eq. A20 provides better regression coefficients to multicyclic conversion data on nonpretreated sorbents [28]. It has the drawback however of yielding, after a large number of cycles, a value for conversion that converges to zero, which is against the empirical observations pointing instead towards an asymptotic decay of conversion to a residual value  $X_r > 0$  [12] (as was effectively predicted by Eq. A16).

The convergence of the multicyclic CaO conversion towards a residual value has been modeled [12] by assuming that the gradual decrease of the surface area tends to zero as  $s_i$  approaches a residual value  $s_r$ . In terms of the surface loss/gain model, this would imply a modification of Eqs. A17-A18 to

$$s_{i+1} - s'_i = -k(s_i - s_r)^2 \quad (\text{A21})$$

$$s'_i - s_i = 0 \quad (\text{A22})$$

$$s_N - 1 = \sum_{i=0}^{N-1} s_{i+1} - s_i = -a \sum_{i=0}^{N-1} (s_i - s_r)^2 \quad (\text{A23})$$

Transformation Eq. A23 to a differential form ( $ds = -k(s - s_r)^2 di$ ) and integration leads to

$$\frac{X_N}{X_0} = \frac{1 + bN}{1 + aN} \quad (\text{A24})$$

which is just another way of writing Eq. 7 with  $a = k(1 - s_r) = k(1 - x_r)$  and  $b = ks_r(1 - s_r) = kx_r(1 - x_r)$ , being  $x_r = X_r/X_0$  and  $X_r$  the conversion residual value. Equation 7 (or its equivalent Eq. A24) generally fits well to most data on conversion of nonpretreated natural limestones ( $b < a$ ) subjected to long-series multicyclic tests [12].

In spite that it might be justified that the surface area evolution of nonpretreated sorbents is mainly governed by sintering, diffusive carbonation may pose in general a contribution to the total conversion, as shown in Fig. 9 from our experimental work. In order not to fully disregard diffusive carbonation, the balance equations

$$\frac{s_{i+1} - s'_i}{s_i} = -a \frac{s_i - s_r}{1 - s_r} \quad (\text{A25})$$

$$\frac{s'_i - s_i}{s_i} = \frac{b}{s_i} \frac{s_i - s_r}{1 - s_r} \quad (\text{A26})$$

$$s_{i+1} - s_i = (-a s_i + b) \frac{s_i - s_r}{1 - s_r} = -k(s_i - s_r)^2 \quad (\text{A27})$$

would serve also to infer Eq. A24. Equation A27 is equivalent to Eq. A21 thus allowing to derive Eq. A24 from a mechanism in which not only sintering but also surface area regeneration by diffusive carbonation is contemplated. Interestingly, Eqs. A25-A26 resemble the equations used in our model for pretreated sorbents. Eq. A25 includes a sintering factor  $a$ , as in the German-Munir model, whereas the regeneration factor  $b/s_i$  in Eq. A26 would be increased if the surface area is decreased with the cycle number or increased if the surface area is increased with the cycle number in accordance with our previous considerations on the evolution of the relative gain of diffusive carbonation. The main difference of Eqs.

A25-A26 with the balance equations in the model proposed in the previous section for pretreated sorbents is that now both sintering/regeneration factors would be attenuated by the multiplying factor  $(s_i - s_r)/(1 - s_r)$  that makes them gradually converge to zero as a residual surface area is approached. Besides, the surface area in the denominator in the left hand side of Eq. A25 and the attenuation factor in the right hand side of this equation is not the surface area after decarbonation  $s'_i$  but the surface area after previous sintering  $s_i$ , which should be the approximate case if  $s'_i \simeq s_i$ , i. e. regeneration is weak ( $b \ll 1$ ). The ratio of gain to loss of surface area is  $(s_{i+1} - s'_i)/(s'_i - s_i) = b/(a s_i) = X_r/X_i$ . In the long term, surface loss/gain are equilibrated and conversion  $X_i$  tends to the residual value  $X_r$ . Regarding the evolution of conversion in the initial cycles, it would strongly depend on the value of the residual conversion  $X_r = X_0(b/a)$ . In the case of nonpretreated sorbents it would be  $X_0 > X_r$ , or equivalently  $b < a$ , which gives rise to a decay of conversion with the cycle number.

It may be of interest to look at the predicted equation for multicyclic conversion if the attenuation factor  $(s_i - s_r)/(1 - s_r)$  in Eqs. A25-A26 were dismissed,

$$\frac{s_{i+1} - s'_i}{s_i} = -a \quad (\text{A28})$$

$$\frac{s'_i - s_i}{s_i} = \frac{b}{s_i} \quad (\text{A29})$$

$$s_{i+1} - s_i = -a s_i + b \quad (\text{A30})$$

By integrating the differential form of Eq. A30 ( $ds = (-a s + b) di$ ), it results

$$\frac{X_N}{X_0} = \frac{b}{a} + \left(1 - \frac{b}{a}\right) e^{-aN} \quad (\text{A31})$$

which depicts also an initial decay ( $b < a$ ) of conversion and a convergence to a residual value  $b/a = X_r$  for large  $N$ . If regeneration were fully neglected ( $b = 0$ ), Eq. A31 takes a form that was already suggested by Wang and Anthony [28] as a potentially useful expression ( $X_N/X_0 = e^{-aN}$ ). Although these authors did not report fittings to experimental data to in fact test its suitability, it may be foreseen that, if the regeneration factor were neglected, Eq. A31 does not fit well to the long-series multicyclic conversion data.

As regards the method of approximating finite differences by infinitesimals in order to carry out summation by means of integration, it must be warned that this approximation is



rigorously valid only if finite differences are actually small, that is  $a$  and  $b$  in Eq. A30 are small. For small  $a$ , it is  $e^{-a} \simeq 1 - a$  and thus Eq. A31 becomes

$$\frac{X_N}{X_0} = \frac{b}{a} + \left(1 - \frac{b}{a}\right) (1 - a)^N \quad (\text{A32})$$

which conforms to Eq. A15 for  $b = 0$ . Note the similarity between Eq. A32 and Eq. A16 that was derived by Abanades [54] from the assumption of a diverse mechanism and that provided good fits to short-series of multicyclic conversion data on nonpretreated sorbents. By taking into account regeneration, and for the first cycles ( $N$  small), it is  $e^{-aN} \simeq 1/(1 + aN)$ . Thus, Eq. A31 conforms to Eq. A24 as might have been expected since, in the first cycles, the attenuation factor in the surface area variation (Eq. A27) is close to one. However, as  $N$  is increased, and thus  $s_i$  diminishes, the attenuation factor is decreased, which slows down the decay of conversion. Consequently, Eq. A31 predicts a more rapid convergence of conversion to its residual value than Eq. A24.

- 
- [1] J. Blamey, E. J. Anthony, J. Wang, and P. S. Fennell, "The calcium looping cycle for large-scale CO<sub>2</sub> capture," *Prog. Energ. Combust. Sci.*, vol. 36, no. 2, pp. 260–279, 2010.
  - [2] C. Dean, J. Blamey, N. Florin, M. Al-Jeboori, and P. Fennell, "The calcium looping cycle for CO<sub>2</sub> capture from power generation, cement manufacture and hydrogen production," *Chemical Engineering Research and Design*, vol. 89, no. 6, pp. 836 – 855, 2011.
  - [3] A. Sanchez-Biezma, J. Ballesteros, L. Diaz, E. de Zarraga, F. Alvarez, J. Lopez, B. Arias, G. Grasa, and J. Abanades, "Postcombustion CO<sub>2</sub> capture with CaO. status of the technology and next steps towards large scale demonstration," *Energy Procedia*, vol. 4, no. 0, pp. 852 – 859, 2011.
  - [4] T. Shimizu, T. HIRAMA, H. Hosoda, K. Kitano, M. Inagaki, and K. Tejima, "A twin fluidbed reactor for removal of CO<sub>2</sub> from combustion processes," *Chemical Engineering Research & Design*, vol. 77, no. A1, pp. 62 – 68, 1999.
  - [5] H. Lu, E. P. Reddy, and P. G. Smirniotis, "Calcium oxide based sorbents for capture of carbon dioxide at high temperatures," *Ind. Eng. Chem. Res.*, vol. 45, pp. 3944 – 3949, 2006.
  - [6] J. C. Abanades, E. J. Anthony, D. Y. Lu, C. Salvador, and D. Alvarez, "Capture of CO<sub>2</sub> from combustion gases in a fluidized bed of CaO," *AIChE J.*, vol. 50, no. 7, pp. 1614–1622, 2004.

- [7] G. Grasa, B. Gonzalez, M. Alonso, and J. C. Abanades, "Comparison of CaO-based synthetic CO<sub>2</sub> sorbents under realistic calcination conditions," *Energ. Fuel.*, vol. 21, no. 6, pp. 3560–3562, 2007.
- [8] B. Arias, J. C. Abanades, and G. S. Grasa, "An analysis of the effect of carbonation conditions on CaO deactivation curves," *Chem. Eng. J.*, vol. 167, no. 1, pp. 255–261, 2011.
- [9] N. Rodriguez, M. Alonso, J. C. Abanades, A. Charitos, C. Hawthorne, G. Scheffknecht, D. Y. Lu, and E. J. Anthony, "Comparison of experimental results from three dual fluidized bed test facilities capturing CO<sub>2</sub> with CaO," *Energy Procedia*, vol. 4, pp. 393 – 401, 2011.
- [10] R. Barker, "Reversibility of the reaction  $\text{CaCO}_3 = \text{CaO} + \text{CO}_2$ ," *J. Appl. Chem. Biotechnol.*, vol. 23, pp. 733 – 742, 1973.
- [11] G. Grasa, R. Murillo, M. Alonso, and J. C. Abanades, "Application of the random pore model to the carbonation cyclic reaction," *AIChE J.*, vol. 55, no. 5, pp. 1246–1255, 2009.
- [12] G. S. Grasa and J. C. Abanades, "CO<sub>2</sub> capture capacity of CaO in long series of carbonation/calcination cycles," *Ind. Eng. Chem. Res.*, vol. 45, no. 26, pp. 8846–8851, 2006.
- [13] L. M. Romeo, Y. Lara, P. Lisbona, and A. Martinez, "Economical assessment of competitive enhanced limestones for CO<sub>2</sub> capture cycles in power plants," *Fuel Processing Technology*, vol. 90, no. 6, pp. 803 – 811, 2009.
- [14] W. Liu, H. An, C. Qin, J. Yin, G. Wang, B. Feng, and M. Xu, "Performance enhancement of calcium oxide sorbents for cyclic CO<sub>2</sub> capture: a review," *Energy & Fuels*, vol. 26, no. 5, pp. 2751–2767, 2012.
- [15] J. M. Valverde, "Ca-based synthetic materials with enhanced CO<sub>2</sub> capture efficiency," *J. Mater. Chem. A.*, vol. 1, p. 447–468, 2013.
- [16] E. P. Reddy and P. G. Smirniotis, "High-temperature sorbents for CO<sub>2</sub> made of alkali metals doped on CaO supports," *J. Phys. Chem. B*, vol. 108, pp. 7794 – 7800, 2004.
- [17] V. Manovic and E. J. Anthony, "Thermal activation of CaO-based sorbent and self-reactivation during CO<sub>2</sub> capture looping cycles," *Environ. Sci. Technol.*, vol. 42, pp. 4170–4174, 2008.
- [18] K. O. Albrecht, K. S. Wagenbach, J. A. Satrio, B. H. Shanks, and T. D. Wheelock, "Development of a CaO-based CO<sub>2</sub> sorbent with improved cyclic stability," *Ind. Eng. Chem. Res.*, vol. 47, p. 7841–7848, 2008.
- [19] V. Manovic, E. J. Anthony, G. Grasa, and J. C. Abanades, "CO<sub>2</sub> looping cycle performance of a high-purity limestone after thermal activation/doping," *Energy & Fuels*, vol. 22, p. 3258

- 3264, 2008.
- [20] V. Manovic, E. J. Anthony, and D. Loncarevic, "CO<sub>2</sub> looping cycles with cao-based sorbent pretreated in at high temperature," *Chemical Engineering Science*, vol. 64, no. 14, pp. 3236 – 3245, 2009.
- [21] N. H. Florin and A. T. Harris, "Reactivity of cao derived from nano-sized CaCO<sub>3</sub> particles through multiple CO<sub>2</sub> capture-and-release cycles," *Chemical Engineering Science*, vol. 64, no. 2, pp. 187 – 191, 2009.
- [22] H. S. S. Z. Chen, M. Portillo, C. J. Lim, J. R. Grace, and E. J. Anthony, "Long-term calcination/carbonation cycling and thermal pretreatment for CO<sub>2</sub> capture by limestone and dolomite," *Energy & Fuels*, vol. 23, p. 1437 1444, 2009.
- [23] V. Manovic, E. J. Anthony, and D. Loncarevic, "Improving the stability of a CaO-based sorbent for CO<sub>2</sub> by thermal pretreatment," *Ind. Eng. Chem. Res.*, vol. 50, p. 6933 6942, 2011.
- [24] B. Arias, J. C. Abanades, and E. J. Anthony, "Model for self-reactivation of highly sintered CaO particles during CO<sub>2</sub> capture looping cycles," *Energy Fuels*, vol. 25, pp. 1926–1930, 2011.
- [25] C. H. Bartholomew, "Sintering kinetics of supported metals: new perspectives from a unifying GPLE treatment," *Applied Catalysis A: General*, vol. 107, no. 1, pp. 1 – 57, 1993.
- [26] R. M. German and Z. A. Munir, "Surface area reduction during isothermal sintering," *Journal of the American Ceramic Society*, vol. 59, no. 9 - 10, p. 379 383, 1976.
- [27] S. E. Wanke and P. C. Flynn, "The sintering of supported metal catalysts," *Catalysis Reviews*, vol. 12, no. 1, pp. 93 – 135, 1975.
- [28] J. Wang and E. J. Anthony, "On the decay behavior of the CO<sub>2</sub> absorption capacity of CaO-based sorbents," *Ind. Eng. Chem. Res.*, vol. 44, pp. 627 – 629, 2005.
- [29] A. I. Lysikov, A. N. Salanov, and A. G. Okunev, "Change of CO<sub>2</sub> carrying capacity of CaO in isothermal recarbonation-decomposition cycles," *Ind. Eng. Chem. Res.*, vol. 46, pp. 4633 – 4638, 2007.
- [30] R. H. Borgwardt, "Sintering of nascent calcium oxide," *Chem. Eng. Sci.*, vol. 44, no. 1, pp. 53–60, 1989.
- [31] M. Alonso, M. Lorenzo, B. Gonzalez, and J. C. Abanades, "Pre-calcination of CaCO<sub>3</sub> as a method to stabilize CaO performance for CO<sub>2</sub> capture from combustion gases," *Energy & Fuels*, vol. 25, no. 11, pp. 5521–5527, 2011.

- [32] B. Stanmore and P. Gilot, "Review - calcination and carbonation of limestone during thermal cycling for CO<sub>2</sub> sequestration," *Fuel Processing Technology*, vol. 86, no. 16, pp. 1707 – 1743, 2005.
- [33] A. B. Fuertes, D. Alvarez, F. Rubiera, J. J. Pis, and G. Marban, "Surface area and pore size changes during sintering of calcium oxide particles," *Chemical Engineering Communications*, vol. 109, no. 1, pp. 73 – 88, 1991.
- [34] J. M. Valverde, A. Perejon, and L. Perez-Maqueda, "Enhancement of fast CO<sub>2</sub> capture by a nano-SiO<sub>2</sub>/CaO composite at Ca-looping conditions," *Environmental Science & Technology*, vol. 46, no. 11, pp. 6401 – 6408, 2012.
- [35] D. Y. Lu, R. W. Hughes, E. J. Anthony, and V. Manovic, "Sintering and reactivity of CaCO<sub>3</sub>-based sorbents for in situ CO<sub>2</sub> capture in fluidized beds under realistic calcination conditions," *J. Environ. Eng.*, vol. 135, no. 6, pp. 404–410, 2009.
- [36] L. Vieille, A. Govin, and P. Grosseau, "Improvements of calcium oxide based sorbents for multiple CO<sub>2</sub> capture cycles," *Powder Technology*, vol. 228, pp. 319 – 323, 2012.
- [37] J. Rouquérol, "L'analyse thermique a vitesse de decomposition constante," *Journal of Thermal Analysis and Calorimetry*, vol. 2, pp. 123 – 140, 1970.
- [38] J. Rouquérol and M. Ganteaume, "Thermolysis under vacuum: essential influence of the residual pressure on thermoanalytical curves and the reaction products," *Journal of Thermal Analysis and Calorimetry*, vol. 11, pp. 201 – 210, 1977.
- [39] J. M. Criado, M. Macias, and A. Macias-Machin, "Analysis of the system CaO-CO<sub>2</sub>-H<sub>2</sub>O for storage of solar thermal energy," *Solar Energy*, vol. 49, pp. 83–86, 1992.
- [40] L. Perez-Maqueda, A. Ortega, and J. Criado, "The use of master plots for discriminating the kinetic model of solid state reactions from a single constant-rate thermal analysis (CRTA) experiment," *Thermochimica Acta*, vol. 277, no. 0, pp. 165 – 173, 1996.
- [41] N. Koga and J. M. Criado, "The influence of mass transfer phenomena on the kinetic analysis for the thermal decomposition of calcium carbonate by constant rate thermal analysis (CRTA) under vacuum," *Int. J. Chem. Kinet.*, vol. 30, p. 737–744, 1998.
- [42] L. A. Perez-Maqueda, J. M. Criado, C. Real, J. Subrt, and J. Bohacek, "The use of constant rate thermal analysis (CRTA) for controlling the texture of hematite obtained from the thermal decomposition of goethite," *J. Mater. Chem.*, vol. 9, p. 1839–1845, 1999.
- [43] P. E. Sanchez-Jimenez, L. A. Perez-Maqueda, J. E. Crespo-Amoros, J. Lopez, A. Perejon,

- and J. M. Criado, “Quantitative characterization of multicomponent polymers by sample-controlled thermal analysis,” *Analytical Chemistry*, vol. 82, no. 21, pp. 8875 – 8880, 2010.
- [44] V. Manovic, J.-P. Charland, J. Blamey, P. S. Fennell, D. Y. Lu, and E. J. Anthony, “Influence of calcination conditions on carrying capacity of CaO-based sorbent in CO<sub>2</sub> looping cycles,” *Fuel*, vol. 88, pp. 1893–1900, 2009.
- [45] R. H. Borgwardt, “Calcium oxide sintering in atmospheres containing water and carbon dioxide,” *Industrial & Engineering Chemistry Research*, vol. 28, no. 4, pp. 493 – 500, 1989.
- [46] H. Chen, C. Zhao, and Q. Ren, “Feasibility of CO<sub>2</sub>/SO<sub>2</sub> uptake enhancement of calcined limestone modified with rice husk ash during pressurized carbonation,” *Journal of Environmental Management*, vol. 93, no. 1, pp. 235 – 244, 2012.
- [47] R. Wu and S. Wu, “Performance of nano-CaCO<sub>3</sub> coated with SiO<sub>2</sub> on CO<sub>2</sub> adsorption at high temperature,” *Huagong Xuebao (Chinese Edition)*, vol. 57, pp. 1722 – 1726, 2006.
- [48] C.-H. Huang, K.-P. Chang, C.-T. Yu, P.-C. Chiang, and C.-F. Wang, “Development of high-temperature CO<sub>2</sub> sorbents made of cao-based mesoporous silica,” *Chemical Engineering Journal*, vol. 161, no. 12, pp. 129 – 135, 2010.
- [49] G. Silcox, J. Kramlich, and D. Pershing, “A mathematical model for the flash calcination of dispersed CaCO<sub>3</sub> and Ca(OH)<sub>2</sub> particles,” *Ind. Eng. Chem. Res.*, vol. 28, p. 155 – 160, 1989.
- [50] C. R. Milne, G. D. Silcox, D. W. Pershing, and D. A. Kirchgessner, “Calcination and sintering models for application to high-temperature, short-time sulfation of calcium-based sorbents,” *Industrial & Engineering Chemistry Research*, vol. 29, no. 2, pp. 139–149, 1990.
- [51] M. Garcia, E. Platero, J. Colinas, and C. Arean, “Variation of surface area during isothermal sintering of mesoporous gamma-alumina,” *Thermochimica Acta*, vol. 90, pp. 195 – 199, 1985.
- [52] S. Bailliez and A. Nzihou, “The kinetics of surface area reduction during isothermal sintering of hydroxyapatite adsorbent,” *Chemical Engineering Journal*, vol. 98, no. 1 - 2, pp. 141 – 152, 2004.
- [53] J. C. Abanades, “The maximum capture efficiency of CO<sub>2</sub> using a carbonation/calcination cycle of CaO/CaCO<sub>3</sub>,” *Chem. Eng. J.*, vol. 90, pp. 303–306, 2002.
- [54] J. C. Abanades and D. Alvarez, “Conversion limits in the reaction of CO<sub>2</sub> with lime,” *Energy & Fuels*, vol. 17, pp. 308 – 315, 2003.

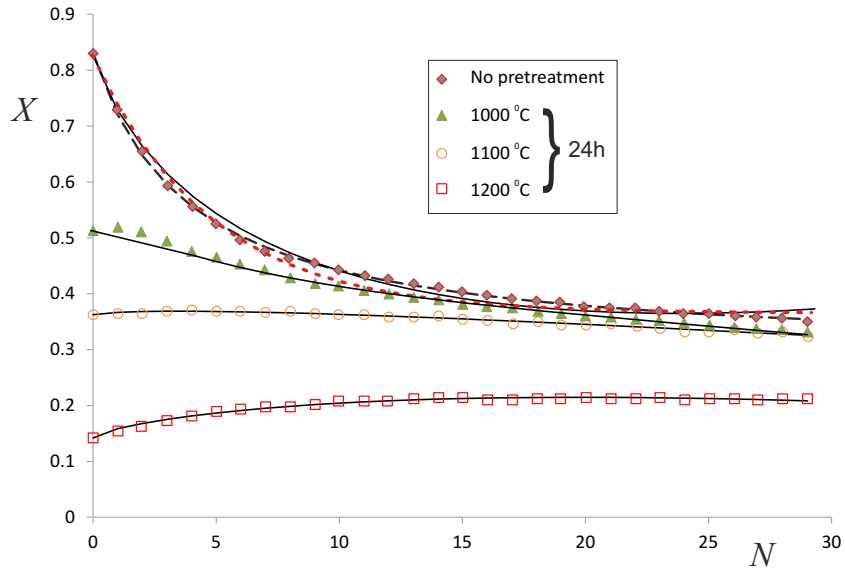


FIG. 1. CaO conversion reported in ref. [19] as a function of the cycle number  $N$  for a powdered natural limestone (LB) and for variable pretreatment temperature. The solid lines are best fit curves from Eq. 10. The dashed/dotted lines represent best fit curves from Eq. 11/12 to data on the nonpretreated sorbent.

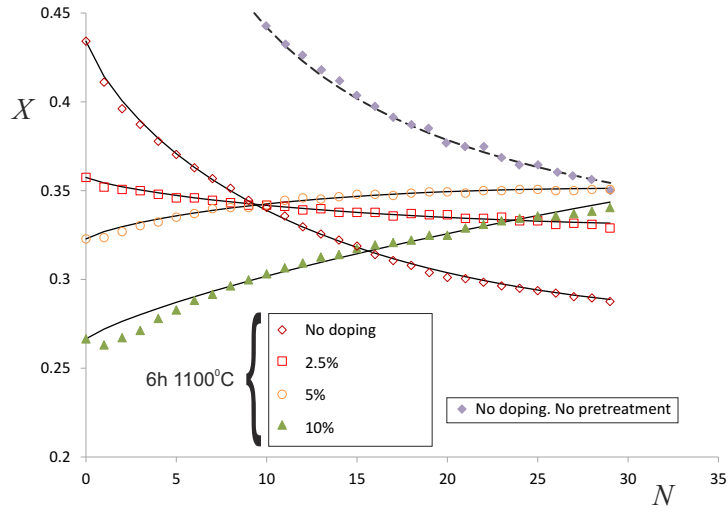


FIG. 2. CaO conversion reported in ref. [19] as a function of the cycle number  $N$  for a natural limestone (LB) and for variable wt% of  $\gamma$ -Al<sub>2</sub>O<sub>3</sub> in mixtures ground and activated for 6 h at 1100°C (the nondoped limestone was not ground); The solid lines are best fit curves from Eq. 10. The dashed line represents the best fit curve from Eq. 11 to data on the nonpretreated and nondoped sorbent.

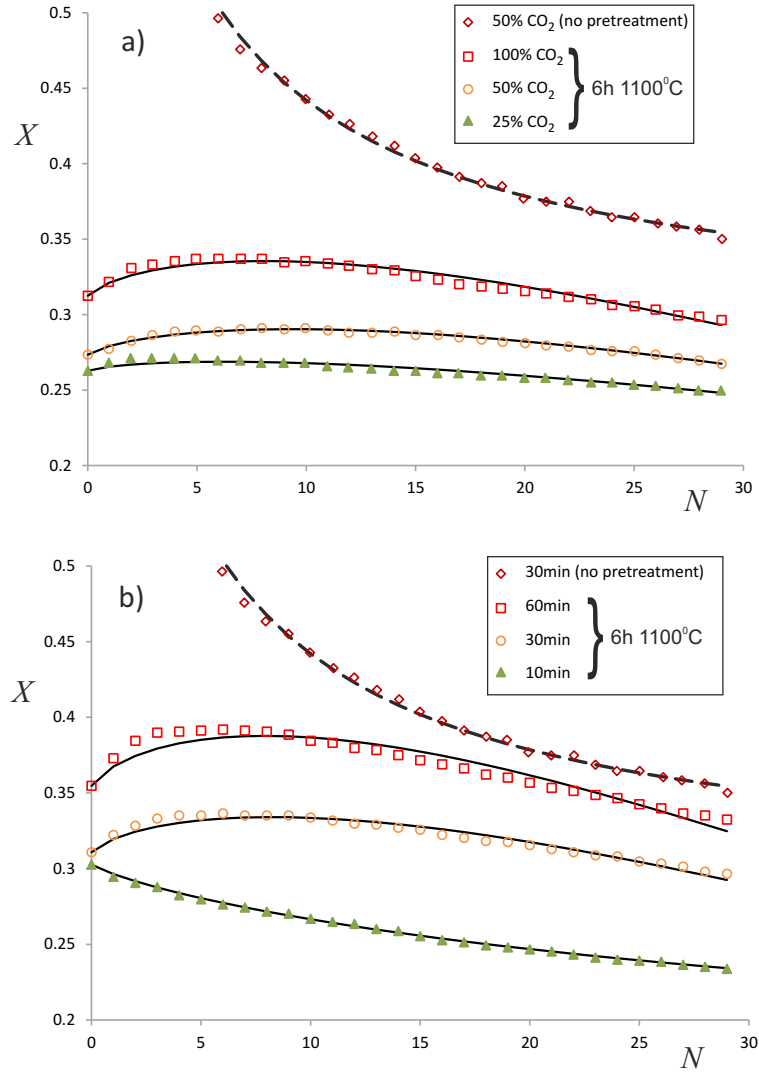


FIG. 3. CaO conversion reported in ref. [19] as a function of the cycle number  $N$  for a powdered natural limestone (LB) and for variable variable carbonation conditions in the CaL cycles as indicated: a) variable % CO<sub>2</sub> ; b) variable carbonation time period. The limestone was pretreated at 1200°C for 6 h. In (b) the CO<sub>2</sub> concentration during carbonation was 100%. The solid lines are best fit curves from Eq. 10. The dashed line represent the best fit curve from Eq. 11 to data on the nonpretreated sorbent subjected to the benchmark looping TGA test (10 min calcination in 100% N<sub>2</sub> and 10 min carbonation in 50% CO<sub>2</sub> -N<sub>2</sub> balance- at 800°C isothermally).



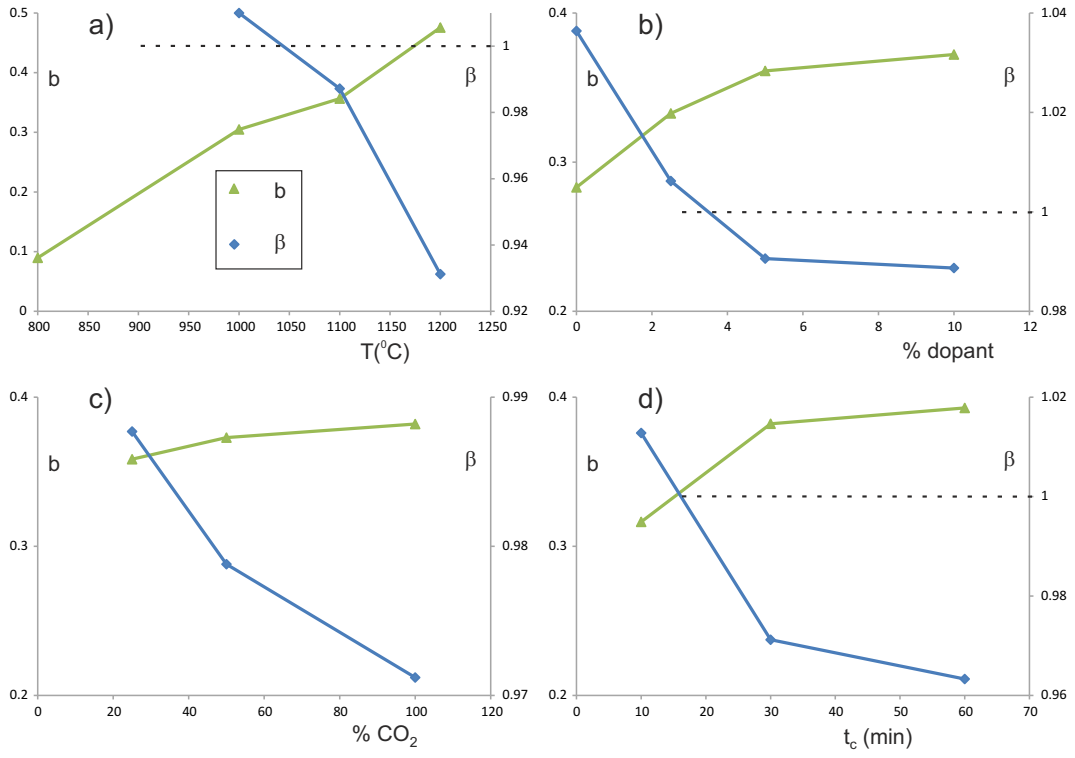


FIG. 4. Regeneration factor  $b$  and regeneration exponent  $\beta$  obtained from the best fits of Eq. 10 to data on CaO conversion of powdered limestones subjected to diverse thermal pretreatments and experimental conditions reported in ref. [19] as detailed in Figs. 1-3. The sintering factor  $a$  is kept fixed ( $a = 0.256$ ) in all the cases.

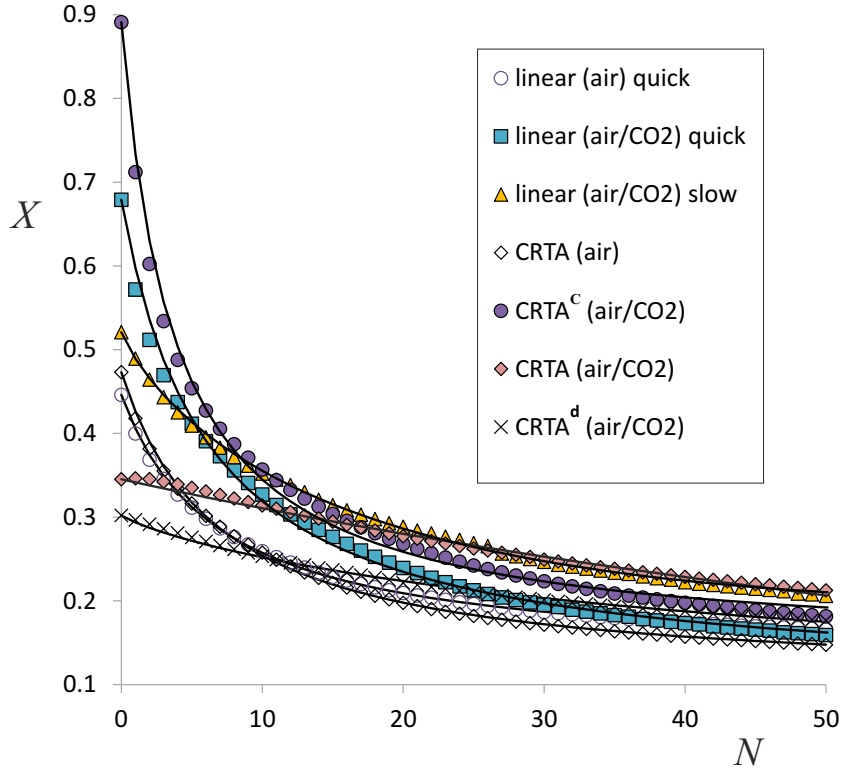


FIG. 5. Conversion of CaO derived from subjecting  $\text{Ca}(\text{OH})_2$  to different preheating programs as indicated in either air or air/ $\text{CO}_2$  atmospheres. In CRTA programs, the temperature is controlled to keep the reactions at a small fixed rate except for decarbonation in air/ $\text{CO}_2$ -CRTA<sup>c</sup> and carbonation in air/ $\text{CO}_2$ -CRTA<sup>d</sup>, which are forced to proceed at a fast rate by a quick linear increment of temperature. The solid lines are best fit curves from Eq. 10-11 according to the parameters shown in table I.

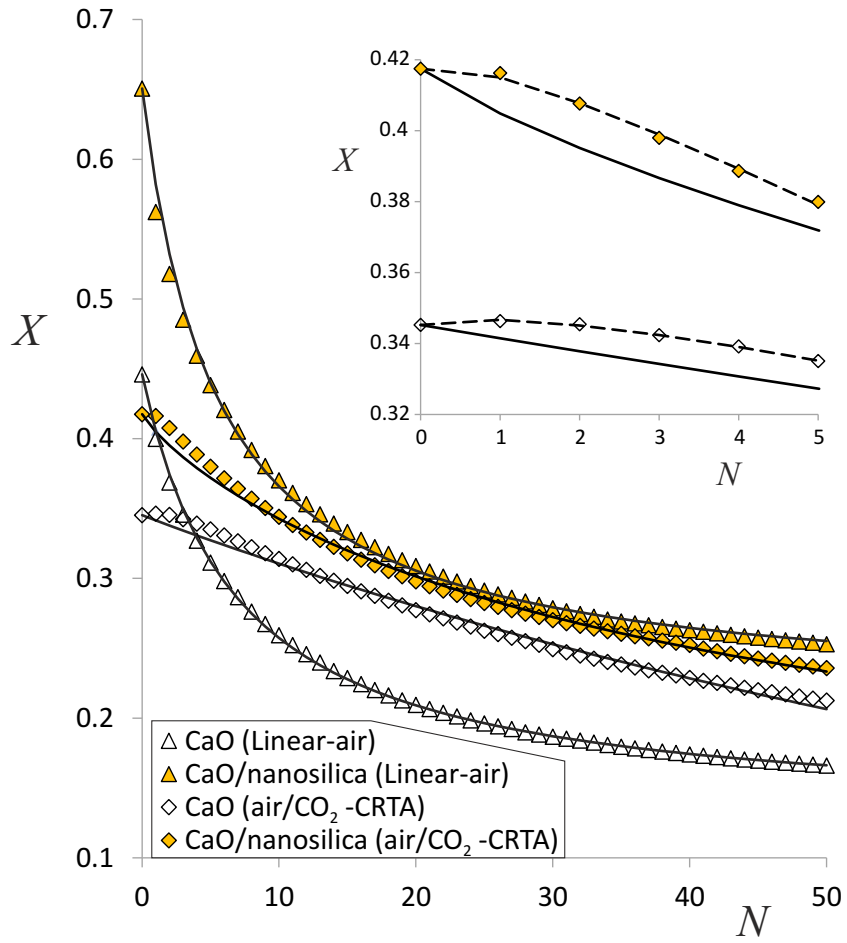


FIG. 6. Conversion of CaO and CaO/nanosilica composite derived from subjecting  $\text{Ca(OH)}_2$  and a  $\text{Ca(OH)}_2/\text{nanosilica}$  dry mixture to linear and air/ $\text{CO}_2$ -CRTA preheating programs as indicated. The solid lines are best fit curves from Eq. 10-11 according to the parameters shown in table I. The inset is a zoom of the first 6 cycles, where dashed lines correspond to the best fits curves from Eq. 10 to conversion data only on these first 6 cycles.

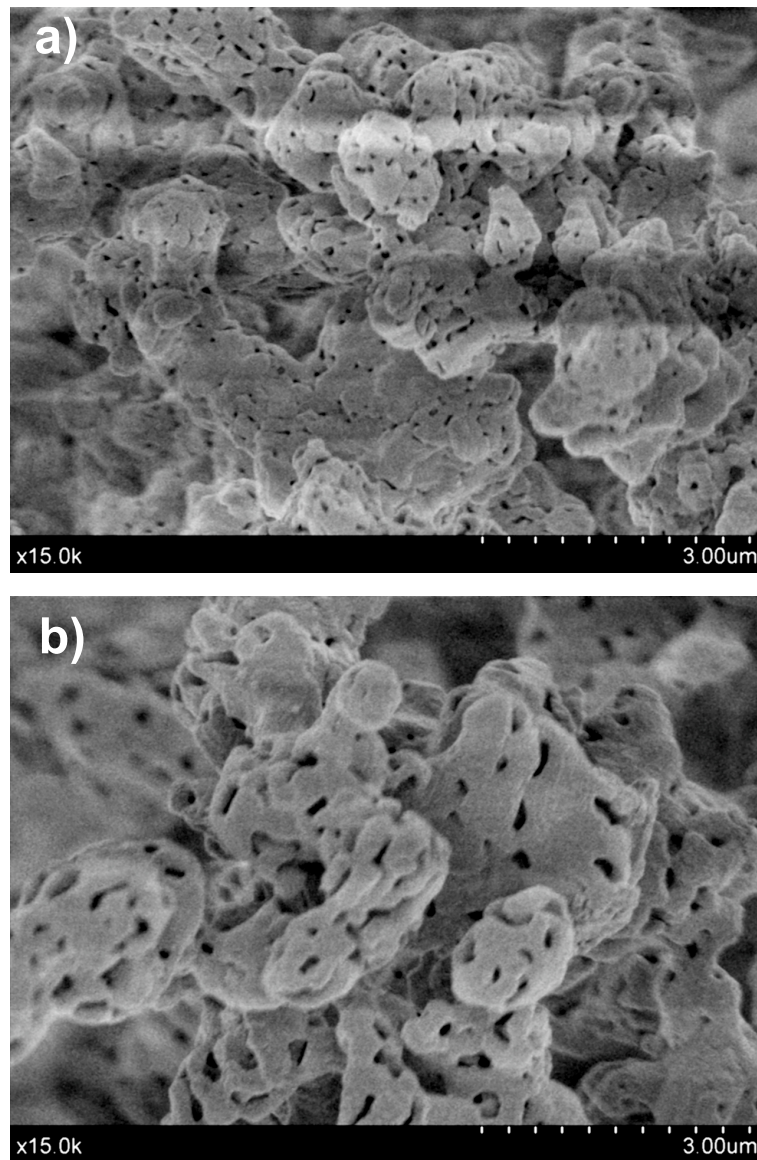


FIG. 7. SEM pictures of CaO samples derived from preheating  $\text{Ca}(\text{OH})_2$  in an air/ $\text{CO}_2$  atmosphere by a linear program (a) and by a CRTA program (b) cooled afterwards in air to avoid carbonation.

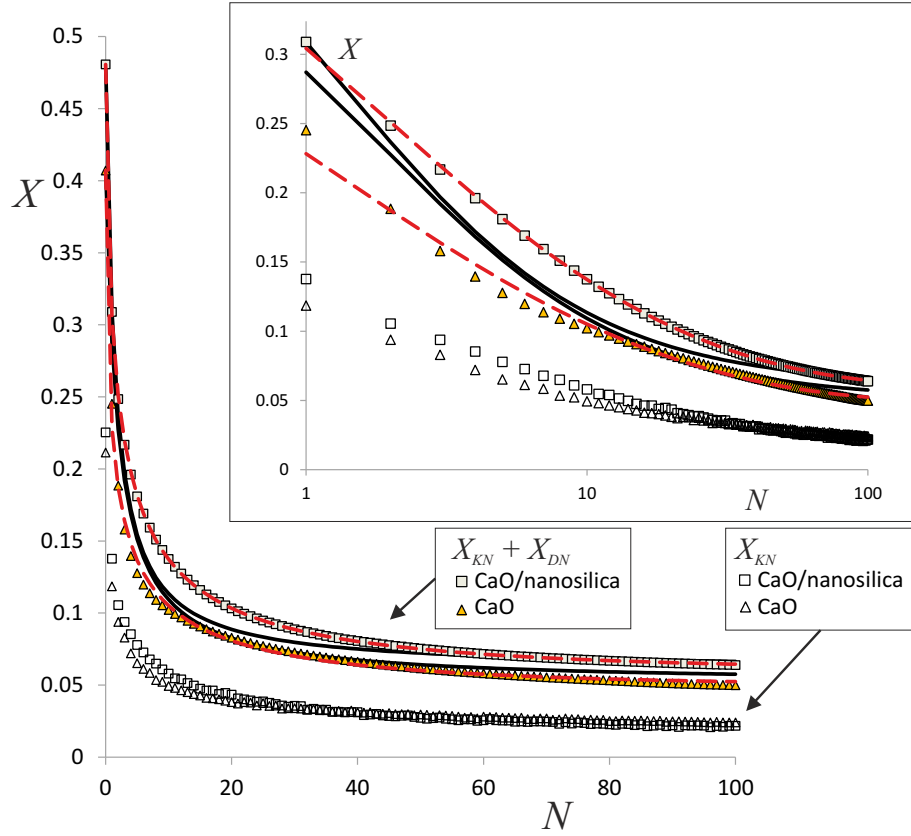


FIG. 8. Conversion of CaO and CaO/nanosilica composite derived from subjecting  $\text{Ca}(\text{OH})_2$  and a  $\text{Ca}(\text{OH})_2/\text{nanosilica}$  dry mixture samples to a quick linear preheating program in air/ $\text{CO}_2$  (90%  $\text{CO}_2$  vol). Looping-calcination is carried out at  $1000^\circ\text{C}$  in air/ $\text{CO}_2$  (90%  $\text{CO}_2$  vol). The solid lines are best fit curves from Eq. 11. The dashed lines are best fit curves from Eq. 17 (table I). Void symbols correspond to CaO conversion data taken just at the end of the fast carbonation phase of each cycle. The inset shows a semi-logarithmic plot to highlight the behavior in the first cycles.

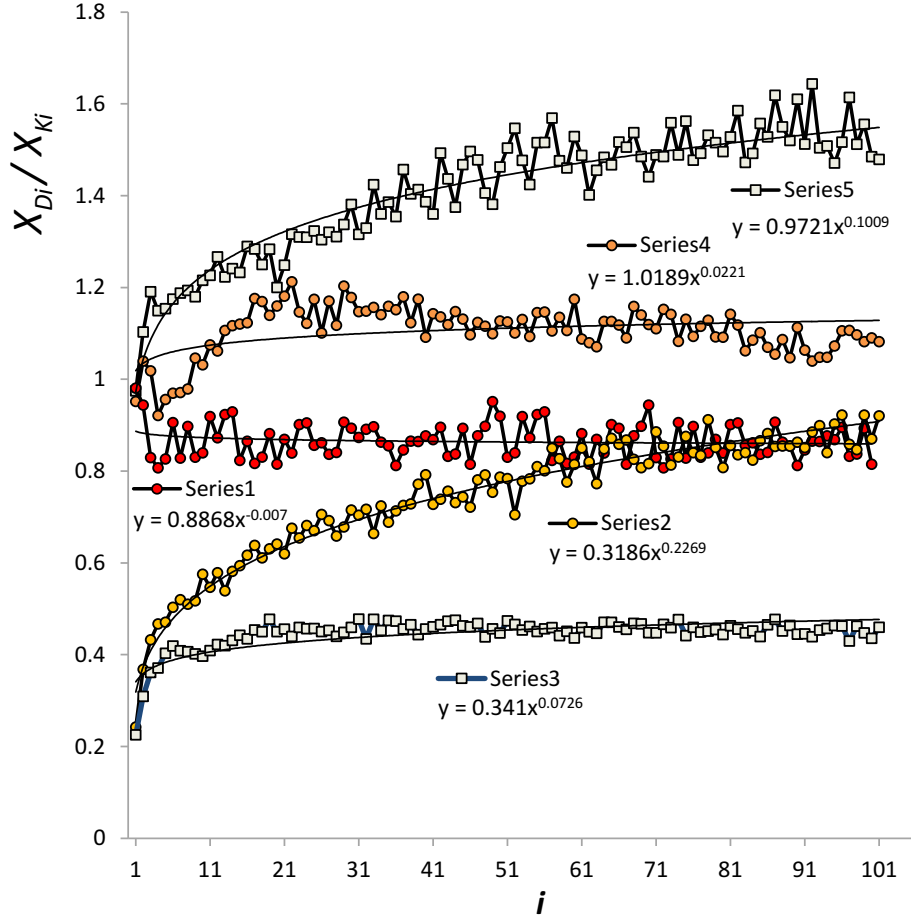


FIG. 9. Ratio of CaO conversion in the diffusive carbonation phase to conversion in the fast kinetic phase for CaO and a CaO/nanosilica composite sorbents tested in our work (derived from diverse preheating programs) as a function of the number of carbonation/calcination cycles. Series 1: CaO (air/CO<sub>2</sub>-CRTA program). Series 2: CaO (air-quick linear program). Series 3: CaO/nanosilica (air-quick linear program). Series 4: CaO (air/CO<sub>2</sub>-quick linear program). Series 5: CaO/nanosilica (air/CO<sub>2</sub>-quick linear program). Looping-carbonation (5 min) under a 15% CO<sub>2</sub>/85% air atmosphere at 650°C and looping-calcination (5min) in either air at 850°C (Series 1, 2, and 3) or in a 90% CO<sub>2</sub>/10% air atmosphere at 1000°C (Series 4 and 5). Power-law fitting curves to the data are plotted and best fit equations are indicated for each series.

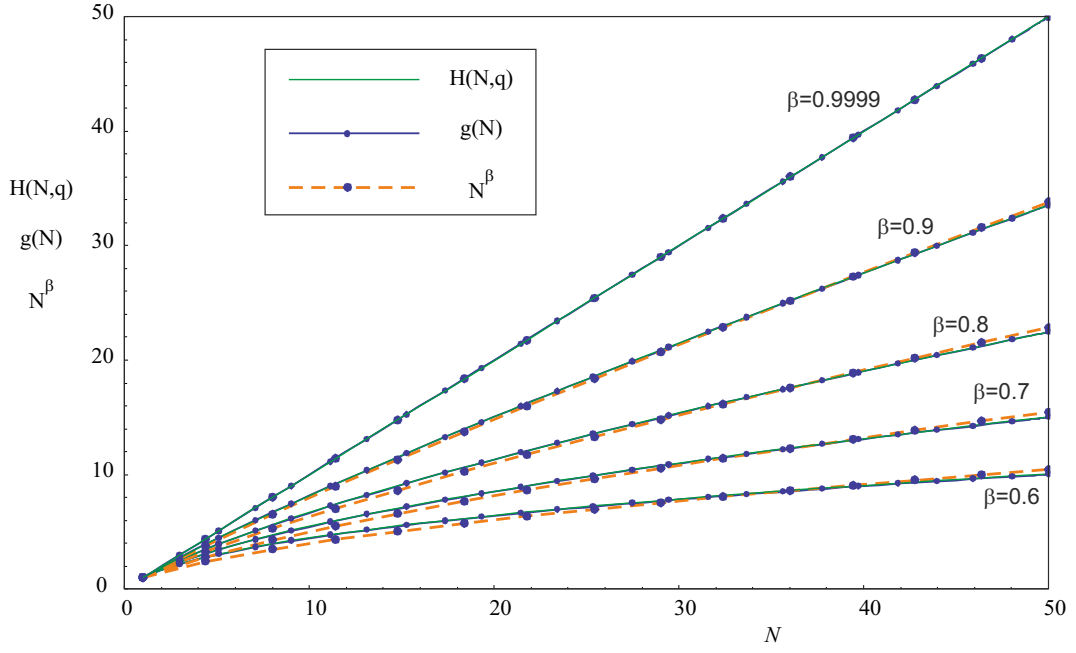


FIG. 10. Harmonic Series function ( $H(N, q)$ ), integral approximation  $g(q) = \frac{1}{1-q} \left[ \left(N + \frac{1}{2}\right)^{1-q} - \left(\frac{1}{2}\right)^{1-q} \right]$ , and power law fit  $N^\beta$  to  $H(N, q)$  ( $q \simeq -1.176 \ln \beta$ ) as a function of  $N$ )